

Design and Biological Activity of (S)-4-(5-{[1-(3-Chlorobenzyl)-2-oxopyrrolidin-3-ylamino]methyl}imidazol-1-ylmethyl)benzonitrile, a 3-Aminopyrrolidinone Farnesyltransferase Inhibitor with Excellent Cell Potency

Ian M. Bell,* Steven N. Gallicchio, Marc Abrams,[†] Douglas C. Beshore, Carolyn A. Buser,[†] J. Christopher Culberson,[‡] Joseph Davide,[†] Michelle Ellis-Hutchings,[†] Christine Fernandes,[†] Jackson B. Gibbs,[†] Samuel L. Graham, George D. Hartman, David C. Heimbrook,[†] Carl F. Homnick, Joel R. Huff, Kelem Kassahun,[§] Kenneth S. Koblan,[†] Nancy E. Kohl,[†] Robert B. Lobell,[†] Joseph J. Lynch, Jr.,^{||} Patricia A. Miller,[†] Charles A. Omer,^{†,^} A. David Rodrigues,[§] Eileen S. Walsh,[†] and Theresa M. Williams

Departments of Medicinal Chemistry, Cancer Research, Molecular Systems, Drug Metabolism, and Pharmacology, Merck Research Laboratories, West Point, Pennsylvania 19486

Received April 5, 2001

The synthesis, structure–activity relationships, and biological properties of a novel series of imidazole-containing inhibitors of farnesyltransferase are described. Starting from a 3-aminopyrrolidinone core, a systematic series of modifications provided **5h**, a non-thiol, non-peptide farnesyltransferase inhibitor with excellent bioavailability in dogs. Compound **5h** was found to have an unusually favorable ratio of cell potency to intrinsic potency, compared with other known FTIs. It exhibited excellent potency against a range of tumor cell lines in vitro and showed full efficacy in the K-rasB transgenic mouse model.

Introduction

Mutation of the GTP-binding protein Ras, a central player in cell signaling pathways that govern cell growth, can lead to cellular transformation and uncontrolled proliferation.¹ The observation that mutant *ras* genes are often found in human tumors suggests that inhibition of Ras function might provide an effective anticancer therapy.^{2,3} Extensive studies on Ras have revealed that a series of posttranslational modifications are required for its biological function, the first step of which is alkylation of a cysteine residue near its C-terminus with a farnesyl group.^{4,5} Thus, the enzyme farnesyltransferase (FTase), which catalyses this step, was identified as a potential target for chemotherapeutic agents. Although subsequent studies have undermined the concept of farnesyltransferase inhibitors (FTIs) as *ras*-directed agents, such inhibitors have shown efficacy in a variety of preclinical cancer models and, more recently, in the clinic.⁶ Our objective was to discover a potent, selective FTI suitable for oral dosing.

A variety of FTIs have been identified, including peptidomimetics derived from the C-terminal CaaX amino acid sequence common to FTase substrates,⁷ natural products,⁸ mimics of farnesyl pyrophosphate (FPP),⁹ and non-peptide non-thiol inhibitors.¹⁰ An example of the latter class of compounds is the *N*-arylpiperazinone template developed at Merck via a

series of modifications to a tetrapeptide lead.¹¹ The central piperazinone moiety in these structures represents a constraint of the original tetrapeptide backbone, and we decided to evaluate other peptidomimetic cyclic constraints. We initially investigated the 3-aminopyrrolidinone template, which has found widespread use in biologically active molecules.^{12,13} We were interested in the inherent β -turn bias of this cyclic constraint, which may mimic the bioactive conformation of some peptide-like inhibitors.¹⁴ The exocyclic amino group in 3-aminopyrrolidinones also offered a convenient divalent synthetic handle to explore substitution patterns that are unavailable to other FTIs such as arylpiperazinones. This report describes our initial investigations on such pyrrolidine-based inhibitors of farnesyltransferase and their evolution to give highly potent antitumor agents.

Chemical Methods

The basic strategy for the synthesis of 3-aminopyrrolidinone farnesyltransferase inhibitors is illustrated in Scheme 1, using the (*S*)-enantiomers as examples. Commercially available amines **1** were coupled with (*S*)-BOC methionine under standard EDC conditions to afford the amides **2**. Unfortunately, for the less nucleophilic anilines **1a** and **1d–f**, these conditions caused loss of stereochemical integrity in the resulting products. For most of the aniline substrates we have investigated, use of PyBOP as the coupling reagent mitigated epimerization and efficiently generated the amide linkage. For 2-chloroaniline (**1d**) and 4-chloroaniline (**1f**), however, even the standard PyBOP conditions gave some epimerization, necessitating a further adaptation of the reaction conditions. Thus, when 5 equiv of 2-chloroaniline was used and the reaction was only allowed to proceed for 30 min at ambient temperature, the desired anilide **2d** was afforded in 86% yield and > 99% ee.

* To whom correspondence should be addressed at the Department of Medicinal Chemistry, Merck Research Laboratories, WP14-2, P.O. Box 4, West Point, PA 19486. Tel: (215) 652-6455. Fax: (215) 652-7310. E-mail: ian_bell@merck.com.

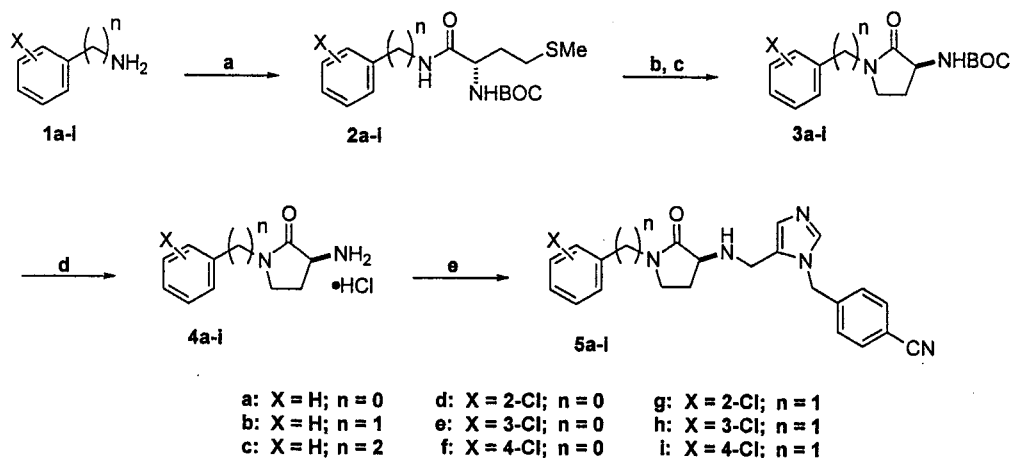
[†] Department of Cancer Research.

[‡] Department of Molecular Systems.

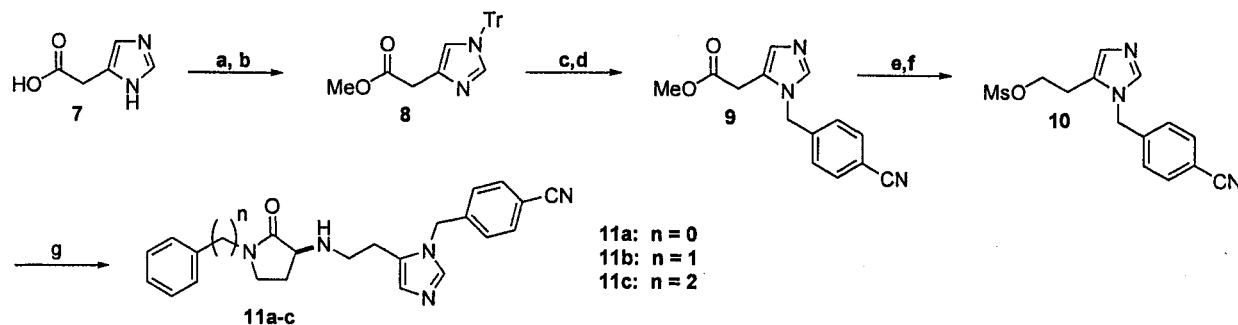
[§] Department of Drug Metabolism.

^{||} Department of Pharmacology.

[^] Current address: Pfizer Inc., 2800 Plymouth Rd., Ann Arbor, MI 48105.

Scheme 1^a

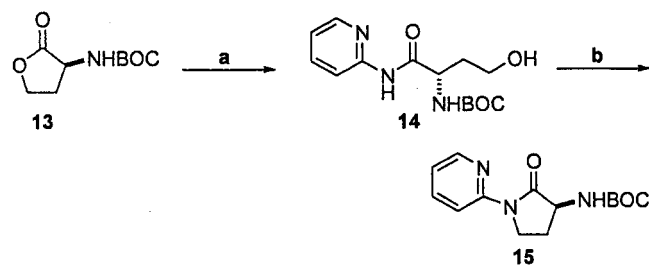
^a Reagents: (a) either (*S*)-BOC methionine, EDC, HOBT, DIEA, and DMF or (*S*)-BOC methionine, PyBOP, DIEA, and CH₂Cl₂; (b) MeI; (c) [(Me)₃Si]₂NLi, THF; (d) HCl, EtOAc; (e) 1-(4-cyanobenzyl)-5-imidazole carboxaldehyde, DIEA, NaCNBH₃, MeOH.

Scheme 2^a

^a Reagents: (a) HCl, TMOF, MeOH; (b) Ph₃CBr, Et₃N, DMF; (c) 4-cyanobenzyl bromide, CH₃CN; (d) MeOH; (e) NaBH₄, MeOH; (f) ClSO₂Me, DIEA, CH₂Cl₂; (g) **4a-c**, DIEA, NaI, DMF.

Construction of the pyrrolidinone ring system was initially accomplished by employing conditions similar to those reported by Freidinger and co-workers.¹⁵ Following treatment of amides **2** with excess iodomethane, the cyclization of resulting sulfonium salts was effected with sodium hydride in DMF-CH₂Cl₂ at 0 °C. However, the isolated BOC-protected aminopyrrolidinones **3** were found to be approximately 15% epimerized. A modified procedure, in which the sulfonium salts were treated with lithium hexamethyldisilylamide in THF at 0 °C, provided the pyrrolidinones **3** in enantiomerically pure form and in good chemical yield (60–95%). Removal of the protecting group with HCl in EtOAc and reductive alkylation of the resulting amine hydrochlorides **4** with 1-(4-cyanobenzyl)-5-imidazole-carboxaldehyde¹¹ using sodium cyanoborohydride in MeOH afforded the desired analogues **5**. Use of alternative conditions that employed sodium triacetoxyborohydride in DCE was complicated by formation of borane complexes with the product, which resulted in difficult purifications and suboptimal yields.

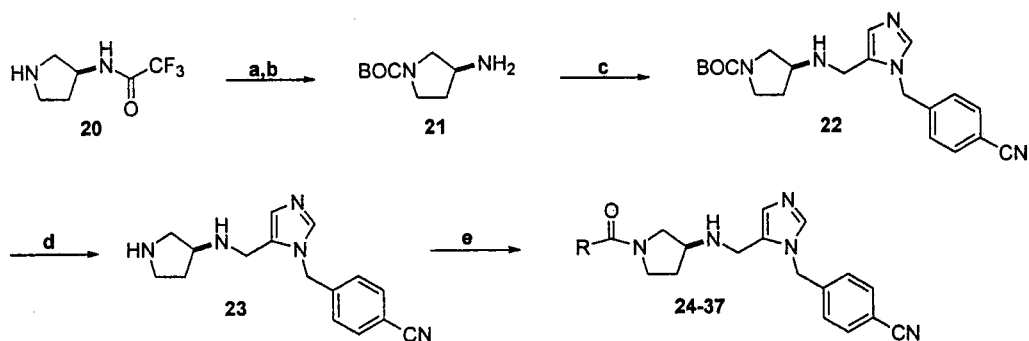
Scheme 2 details the preparation of homologues **11**. In analogy with previous work,¹⁶ imidazole-4-acetic acid (**7**) was esterified and regioselectively protected with triphenylmethyl bromide to give the imidazole **8**. Alkylation of **8** with 4-cyanobenzyl bromide¹⁶ in acetonitrile at 50 °C afforded the imidazolium salt that, following methanolic removal of the trityl group, led to the hydrogen bromide salt of **9**. Reduction of **9** with sodium borohydride in MeOH gave the alcohol cleanly and

Scheme 3^a

^a Reagents: (a) 2-aminopyridine, AlMe₃, CH₂Cl₂; (b) *n*-Bu₃P, DBAD, THF.

conversion to the mesylate **10** proceeded as expected. Finally, alkylation of amines **4a-c** with freshly prepared mesylate **10** in DMF, in the presence of DIEA and sodium iodide, afforded the desired analogues **11** in moderate yield (20–40%).

A small number of analogues containing heterocyclic rings could not be prepared by the previously described sulfonium salt route due to incompatibility with iodomethane. Therefore, an alternative design strategy was developed in our laboratory, and an example is shown in Scheme 3.¹⁷ Treatment of 2-aminopyridine with trimethylaluminum in CH₂Cl₂ and then reaction of the resulting aluminum amide with (*S*)-BOC homoserine lactone provided amide **14**. The intermediate **14** was cyclized under Mitsunobu conditions¹⁸ using tri-*n*-butyl phosphine and di-*tert*-butyl azodicarboxylate in THF to afford the heterocyclic pyrrolidinone **15** in good

Scheme 4^a

For the definition of R, see Table 3

^a Reagents: (a) (BOC)₂O, DIEA, DMF; (b) NaOH, THF, H₂O; (c) 1-(4-cyanobenzyl)-5-imidazole carboxaldehyde, HOAc, NaCNBH₃, MeOH; (d) HCl, EtOAc; (e) RCO₂H, HOBT, EDC, DMF.

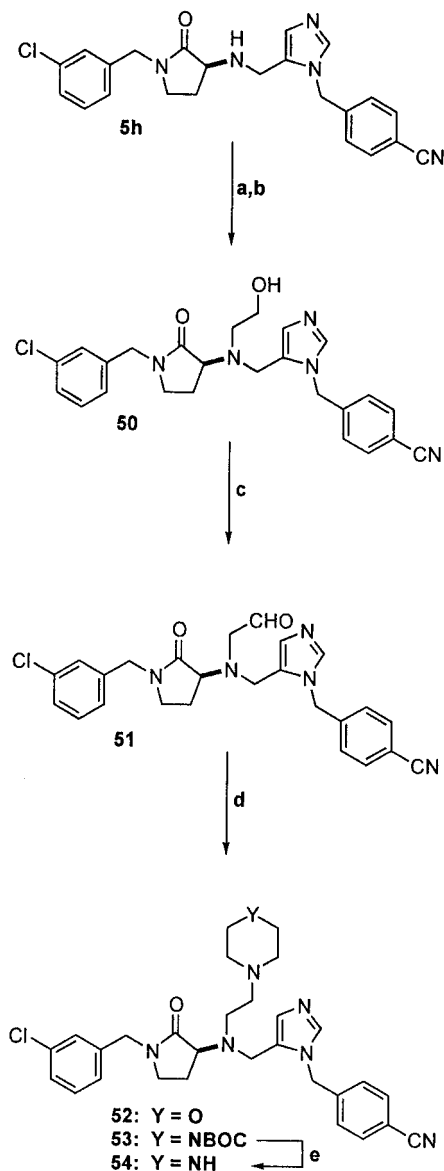
yield and high enantiomeric excess (95% yield, >99% ee). The 1-heterocyclic pyrrolidinones generated in this fashion were converted to the desired compounds, in analogy with the route described in Scheme 1.

To rapidly explore SAR of the substituent on the pyrrolidine nitrogen, a related series of acyl pyrrolidines was investigated (Scheme 4). Ample quantities of pyrrolidine **23** were prepared using the straightforward route shown, and treatment of **23** with a variety of carboxylic acids under EDC-mediated coupling conditions afforded the analogues **24–37**. This strategy was also applied to the synthesis of a small library, in which a simple aqueous workup procedure afforded the final products in good to excellent purity (70–99%).

Transformation of the 3-aminopyrrolidinone secondary amino group into the corresponding tertiary amine was accomplished by reductive alkylation of amines **5b** or **5h** with various aldehydes to give compounds **38–49**. The synthetic details of two related tertiary amine analogues, **52** and **54**, are shown in Scheme 5. Incorporation of the acetaldehyde subunit in structure **51** was accomplished by reductively alkylating amine **5h** with 2-(*tert*-butyldimethylsilyloxy)acetaldehyde,¹⁹ followed by removal of the silyl group and subjecting the resulting alcohol to classical Swern conditions.²⁰ Reductive amination of aldehyde **51** with either morpholine or BOC-piperazine led to compounds **52** and, after deprotection, **54**.

Biological Methods

Compounds were tested as inhibitors of FTase *in vitro* using purified recombinant human enzyme²¹ to catalyze the reaction between [1-³H]FPP and a recombinant protein substrate containing the K-Ras C-terminus (PD CVIM²²). Incorporation of the labeled farnesyl group into the protein substrate was quantitated by precipitation of total protein with acid and scintillation counting.^{9a} The inhibitory activity of the compounds is reported as an IC₅₀ value, the concentration of inhibitor required to reduce radiolabel incorporation by 50% compared with an uninhibited control experiment. The final concentration of organic solvent (either methanol or DMSO) in the assay incubations was 0.5 vol %. Inhibition of geranylgeranyl-protein transferase type I (GG-Tase-I) was evaluated in a scintillation proximity assay using enzyme prepared as described previously.²³ The enzymatic reaction between [1-³H]GGPP and a biotiny-

Scheme 5^a

^a Reagents: (a) 2-(*tert*-butyldimethylsilyloxy)acetaldehyde, NaCNBH₃, HOAc, MeOH; (b) TBAF, THF; (c) oxalyl chloride, DMSO, TEA, CH₂Cl₂; (d) R₂NH, HOAc, NaCNBH₃, MeOH; (e) HCl, EtOAc.

lated peptide that represents the C-terminus of the K4B-Ras protein (biotinyl-GKKKKKSKTKCVIM) was carried out in the presence of phosphates (5 mM ATP)

and varying concentrations of inhibitor.²⁴ Reaction was terminated by addition of streptavidin scintillation proximity assay beads (Amersham), and the mixtures were subsequently analyzed by scintillation counting, reporting IC₅₀ values as described above. For the FTase and GGTase inhibition assays, most determinations were carried out at least twice and the repeats were generally within 2-fold of the original value. Standard deviations from the mean value are shown for IC₅₀ values determined three or more times.

The affinity of compounds for the I_{Kr} channel was evaluated in radioligand competition experiments analogous to [³H]dofetilide binding assays.²⁵ The human ERG potassium channel was stably expressed in 293 embryonic kidney cells,²⁶ and plasma membrane fractions prepared from these cells were used for competition experiments with [³⁵S]-MK499 (L-706,000).²⁷ Results are reported as inflection points (IP) for the test compounds to inhibit binding of the radioligand. Most determinations were carried out at least twice and the repeats were generally within 2-fold of the original value. Standard deviations from the mean value are shown for IP values determined three or more times.

Inhibition of FTase in cells was evaluated by a cell-based radiotracer assay for farnesyltransferase inhibition (CRAFTI), in which the concentration of compound required to displace 50% of a potent, radiolabeled FTI from FTase in cultured H-*ras*-transformed Rat1 cells was determined. This radiotracer, [¹²⁵I]-4-{{5-((2*S*)-4-(3-iodophenyl)-2-[2-(methylsulfonyl)ethyl]-5-oxopiperazin-1-yl)methyl}-1*H*-imidazol-1-yl)methyl}benzotrile, has ~50 000 high-affinity binding sites (apparent *K*_d ~ 1 nM) in the Rat1 cell line. The nonspecific binding signal, determined by the addition of a 1000-fold excess of unlabeled competitor FTI, is typically 5-fold lower than the specific binding signal. The assay provides comparable results using a variety of cell lines and is performed as follows. Cells are seeded at 200 000 cells per well in 24-well tissue culture plates and cultured for 16 h. The radiotracer (~300–1000 Ci/mmol) is diluted into culture media to a concentration of 1 nM, along with the desired concentration of test compound, and then added to the cell monolayers. The test compound was diluted in DMSO and the final concentration of DMSO in the assay was 0.1 vol %. After a 4 h incubation at 37 °C, the cells are briefly rinsed with phosphate-buffered saline, removed from the culture plate by trypsinization, and then subjected to γ -counting using a CobraII γ -counter (Packard Instrument Co.). Dose-inhibition curves and IC₅₀ values are derived from a four-parameter curve-fitting equation using SigmaPlot Software. In cases where determinations were carried out at multiple times, the repeats were generally within 2-fold of the original value. Standard deviations from the mean value are shown for IC₅₀ values determined three or more times.

The inhibition of anchorage-independent cell growth on poly(HEMA)-coated microtiter plates for H-*ras*-transformed Rat1 cells and a variety of human tumor cell lines was assayed using conditions analogous to those described in the literature.²⁸ Anchorage-independent growth inhibition was also evaluated for Rat1 cells transformed by oncogenic H-*ras*, K-*ras*, or H-*ras*-CVLL, suspended in soft agar. The concentration of FTI

required to inhibit cell growth 90% under the standard assay conditions²⁹ is reported as an IC₉₀ value. The cytotoxic endpoint for compounds was evaluated for normal cultured Rat1 cells by measuring the highest concentration of drug compatible with 80% cell survival, as determined by MTT staining.³⁰

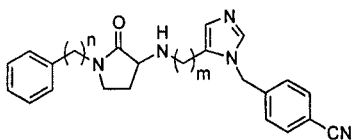
In vivo antitumor efficacy was evaluated in the mouse mammary tumor virus-K-*rasB* transgenic mouse model, with the compound being administered by subcutaneous infusion from an Alzet osmotic minipump. A full description of this efficacy model and experimental conditions has been published elsewhere.³¹ Pharmacokinetic studies of compound **5h** in dogs were performed according to standard protocols. The compound was dosed to three dogs either intravenously (1 mg/kg in DMSO) or orally (3 mg/kg in 0.5% methocellulose suspension), and the resulting plasma levels were quantitated by LCMS. Class III electrophysiologic activity was assessed in anesthetized dogs with the compound of interest being administered by intravenous infusion in an escalating-dose protocol. Plasma levels of compound and electrocardiogram data were determined before and during the infusions. The effects on the QT_c interval (the duration from the start of the QRS complex to the end of the T wave, corrected for heart rate) were correlated with drug concentrations in plasma to yield an EC₁₀ value, the concentration of compound which prolonged the QT_c interval by 10%.

Results and Discussion

Our initial conception of 3-aminopyrrolidinone-based FTIs consisted of this central heterocyclic template positioned between the previously identified cyanobenzylimidazole¹⁶ moiety and a hydrophobic aryl ring, in analogy with piperazinone-based inhibitors of the enzyme.¹¹ We thought that investigation of such a system would allow an evaluation of the potency and other properties of 3-aminopyrrolidinone FTIs with respect to their piperazinone counterparts. A systematic study to vary the length of the linkers between these two end groups and the pyrrolidinone unit, as well as to explore any stereochemical preference of FTase for such structures, was undertaken, and the results are summarized in Table 1.

As shown, the only compounds that exhibited IC₅₀ values against FTase below 100 nM were those in which a methylene linker connected the imidazole to a 1-benzyl- or 1-phenyl-substituted aminopyrrolidinone (compounds **5a**, **5b**, and **6b**). Among the inhibitors with this substitution pattern, FTase exhibited a modest preference for the (*S*)-enantiomer (compare, for example, compounds **5b** and **6b**). This stereochemical preference proved to be quite general for the more potent pyrrolidine-containing inhibitors of this structural class (data not shown), and the remaining tables only detail the (*S*)-enantiomers. The set of backbone variants described in Table 1 was counterscreened against the related enzyme GGTase-I. While all the compounds were selective for FTase vs GGTase-I, the most potent inhibitors of this latter enzyme contained an ethylene linker in the backbone between the imidazole and amino groups and exhibited a preference for a longer linker to the phenyl probe (see compounds **11a**–**11c**).

Evaluation of the most potent FTIs (compounds **5a**, **5b**, and **6b**) in the cell-based assay for binding to FTase

Table 1. 3-Aminopyrrolidinone Inhibitors of FTase: Backbone Modifications

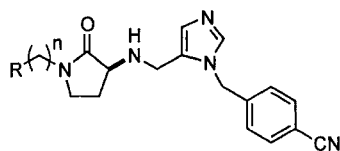
Compound	n	m	stereo ^a	FTase IC ₅₀ (nM) ^b	GGTase IC ₅₀ (nM) ^b	CRAFTI IC ₅₀ (nM) ^b	hERG IP (nM) ^b
5a	0	1	S	74 ± 25 (4)	46,000 (2)	27 (1)	
6a	0	1	R	200 (1)	41,000 (1)		
5b	1	1	S	29 ± 11 (4)	40,000 ± 6,900 (6)	5.7 (1)	7,200 ± 2,700 (3)
6b	1	1	R	49 (2)	46,000 (1)	21 (1)	
5c	2	1	S	230 (2)	48,000 (2)		
6c	2	1	R	250 (1)	31,000 (2)		
11a	0	2	S	280 (1)	14,000 (2)	150 (1)	
12a	0	2	R	120 (2)	16,000 (2)		
11b	1	2	S	270 (1)	7,400 (2)		
12b	1	2	R	250 (1)	11,000 (2)		
11c	2	2	S	240 (2)	2,800 (2)		
12c	2	2	R	380 (1)	1,500 (2)		

^a Stereochemistry at C-3 of pyrrolidinone. ^b Number of replicates used to determine IC₅₀ values shown in parentheses.

(CRAFTI) provided a surprise: the IC₅₀ values were 2–5-fold lower in the cell-based assay than in the in vitro enzyme assay. This observation contrasted with most compounds tested in these assays, such as the *N*-arylpiperazinones,³² for which the inhibitory activity in the cell assay was at best equivalent to the intrinsic activity against the enzyme, and it suggests that these aminopyrrolidinones are unusually effective in terms of cell activity. While this result was unexpected, it should be noted that the assays are measuring different endpoints under different conditions. The FTase inhibition assay measures incorporation of a labeled farnesyl group into a CaaX-containing protein, while in the cell-based assay the displacement of a potent radioligand from the FTase active site is analyzed. Moreover, the CRAFTI assay superimposes a number of other factors onto the simple competition experiment, such as the

activity of the P-glycoprotein pump (vide infra). The observation of lower IC₅₀ values in the cell-based assay compared to the intrinsic enzyme assay simply indicates that the compounds are, for a given level of intrinsic inhibitory activity, unusually potent in cells.

The most potent analogue (**5b**) had an intrinsic IC₅₀ value of 29 nM against FTase but was 5 times more potent in the cell-based assay (CRAFTI IC₅₀ = 5.7 nM). The ability of **5b** to inhibit binding of the radioligand to FTase in cells correlated well with its effects on the growth of *H-ras*-transformed Rat1 cells on poly(HEMA)-coated microtiter plates.²⁸ Specifically, the growth of such cells was inhibited by **5b** with an IC₅₀ value of 33 nM. While this IC₅₀ for growth inhibition is not remarkable in itself, it is noteworthy that it is essentially equivalent to the intrinsic IC₅₀ of compound **5b** against FTase, again demonstrating an unusually favorable

Table 2. 3-Aminopyrrolidinone Inhibitors of FTase

Compound	n	R	FTase IC ₅₀ (nM) ^a	GGTase IC ₅₀ (nM) ^a	CRAFTI IC ₅₀ (nM) ^a	hERG IP (nM) ^a
5d	0		1.5 (2)	42,000 ± 3,800 (3)	14 (1)	
5e	0		8.4 (2)	6,500 (2)	30 (1)	
5f	0		21 (2)	11,000 (2)	30 (1)	
5g	1		5.2 (2)	11,000 ± 4,100 (5)	2.7 (1)	
5h	1		1.9 ± 0.6 (4)	3,400 (2)	0.52 ± 0.13 (3)	440 ± 22 (3)
5i	1		25 (1)	15,000 (2)	53 (1)	
16	0		370 (2)	36,000 (1)		
17	0		85 (2)	> 20,000 (1) ^b	240 (1)	
18	0		43 (1)	> 20,000 (1) ^b	200 (2)	3,200 (2)
19	0		10 (2)	> 20,000 (1) ^b	9.5 (1)	8,200 (2)

^a Number of replicates used for determination shown in parentheses. ^b IC₅₀ determined with preincubation of inhibitor and enzyme.

ratio of cell potency to intrinsic potency. This interesting property encouraged us to pursue analogues of compound **5b** and the corresponding anilide **5a**.

The first analogues of **5a** and **5b** to be examined explored the effects of simple chloro substitution around

the phenyl hydrophobe, and the results of this SAR study are detailed in Table 2. For the anilides (**5d–f**) intrinsic potency against the enzyme decreased in the order 2-Cl > 3-Cl > 4-Cl. Thus, the 2-chloroanilide **5d** was found to be the best inhibitor of FTase both

intrinsically ($IC_{50} = 1.5$ nM) and in the cell-based binding assay ($IC_{50} = 14$ nM), although the addition of this substituent reduced the compound's ability to function in the cell assay. Attenuated performance in cells is often attributed to increased protein binding or poorer cell penetration properties, although the additional chlorine atom in **5d** seemed to have little effect on the compound's lipophilicity (for **5d**, $\log P = 1.75$, compared with the des-chloro analogue **5a**, $\log P = 1.87$) or human serum protein binding (for **5d**, free fraction = 25%, compared with **5a**, free fraction = 22%). These observations indicate that the differences in relative cell potency were not simply due to changes in physical properties or protein binding but probably involved other factors (vide infra).

A parallel series of substituted 1-benzylpyrrolidinones was also examined (compounds **5g–i** in Table 2). In terms of intrinsic potency against FTase, the 4-chloro analogue **5i** was equipotent with the unsubstituted version **5b**, while the 2-chloro analogue **5g** was about 6-fold more potent and the 3-chloro compound **5h** 15-fold more potent than **5b**. The chloro-substituted analogues in Table 2 were counterscreened against GG-Tase-I and showed uniformly good selectivity against this related enzyme. The relative levels of intrinsic and cellular inhibition of FTase varied somewhat for the three chlorobenzyl compounds, but gratifyingly, the most potent analogue, **5h**, had a 4-fold lower IC_{50} in the cell-based assay, consistent with the results observed for the compounds in Table 1. Many factors control the ability of a compound to function in a cell-based assay, such as penetration of the cell membrane, protein binding, chemical stability, and maintenance of suitable concentrations in the relevant cellular compartments, so it is difficult to explain such phenomena simply. A well-known factor in cell potency is the P-glycoprotein pump (PGP), which can expel a variety of compounds from the cytosol and render them less functional in cells.³³ Indeed, the radioligand used for the CRAFTI assay is known to be a substrate for PGP.³⁴ When the CRAFTI assay was performed in the presence of 20 μ M verapamil, which effectively blockades the P-glycoprotein pump,³³ the IC_{50} value of **5h** shifted 5-fold to 2.5 nM. This observation is consistent with the idea that **5h** is not a good substrate for PGP relative to the radioligand, and this may explain why 3-aminopyrrolidinones such as **5h** seem to be particularly cell potent. Since PGP activity is a common cause of resistance to chemotherapeutics in cancer cells, we were encouraged by the fact that compound **5h** seemed to be a relatively poor substrate for this pump.

Molecular modeling studies provided a structure of **5h** docked in the FTase active site, using the protein structure determined by X-ray crystallographic studies on a ternary enzyme complex (see Figure 1). As shown, the key interactions are believed to be ligation of the catalytic zinc by the imidazole moiety, interaction of the cyanophenyl group with the farnesyl chain, and binding of the chlorophenyl ring in a hydrophobic pocket defined by three aromatic residues. The pyrrolidinone ring does not appear to be making any important interactions with the protein and is oriented toward the solvent.

One issue that has gained considerable attention in the field of drug discovery recently is the potential for

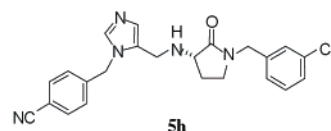
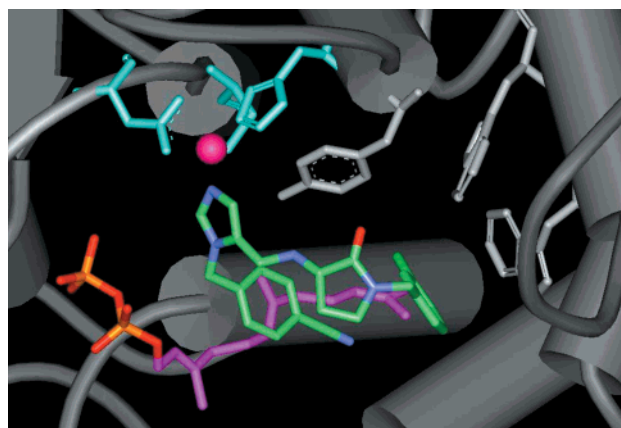


Figure 1. Docked structure of compound **5h** in the FTase active site. The α -subunit has been removed for clarity. The farnesyl group of FPP is shown in magenta. The side chains that ligate the zinc (Asp297, Cys299, and His362) are colored pale cyan, and a hydrophobic pocket defined by the Trp102, Trp106, and Tyr361 side chains (light gray) is indicated. Conformers of the FTI were generated using JCG⁴³ within the FTase active site as determined by Beese et al.⁴⁴ The conformations were subsequently minimized within the rigid active site with the MMFF force field using Macromodel.⁴⁵ During the energy minimization, the imidazole nitrogen which is coordinated to the zinc was held fixed, and a distance-dependent dielectric constant of 2.0 was employed. The resulting conformations were ordered by energy, and a representative structure is shown.

QT_c interval prolongation, often associated with blockade of cardiac ion channels.³⁵ Indeed, prolongation of the QT_c interval has been observed with Merck's clinical candidate FTI during Phase I studies.⁶ These concerns led us to counterscreen compounds against the human I_{Kr} potassium channel, which has been implicated in QT_c effects,^{35,36} and **5h** was found to have moderate binding affinity at this channel (hERG IP = 440 nM). Furthermore, analysis of compound **5h** in anesthetized dogs revealed that it caused 10% prolongation of the QT_c interval at a plasma level of 2.5 μ M. Studies on the parent compound **5b** showed that it had a lower affinity for the ion channel (hERG IP = 7200 nM; see Table 1) but that it nonetheless caused a 10% increase in the QT_c interval in dogs at a 2-fold lower plasma level (1.2 μ M). The lack of absolute correlation between the hERG channel binding affinity of these two compounds and their class III activity in dogs may be due to species variations between the human and canine ion channels, activity of the compounds at other ion channels, or possibly to differential protein binding of **5b** and **5h**. Whatever the explanation for these discrepancies, it was clear that even micromolar affinity for this ion channel might correlate with undesirable cardiac effects, and we sought modifications that would alleviate such activity.

It seemed possible that incorporation of polar functionality at key positions in these FTIs might reduce their affinity for the I_{Kr} channel while having little effect on their potency against FTase, so a number of basic heterocycles were investigated as alternatives to the

phenyl groups in compounds such as **5a**. Table 2 illustrates a number of these analogues (compounds **16–19**), and it was apparent that such modifications could significantly reduce affinity for FTase (compare **16** with **5a**). Compound **19** illustrated, however, that this strategy may have some merit, since it combined good potency against the enzyme with good cell penetration and attenuated ion channel binding. We decided that it may be possible to discover heterocyclic endgroups that were consistent with good enzyme inhibition in the absence of significant binding in the hERG assay by using a different template that facilitated rapid exploration of such substituents.

A related series of compounds, in which the pyrrolidinone carbonyl group is migrated out of the ring to give 1-acylpyrrolidine-based structures, offered one way to approach this problem. A number of these pyrrolidine-based FTIs were synthesized and they possessed moderate activity against FTase (see Table 3). Thus, the pyrrolidine analogue **24** is a simple isomer of structure **5b** (Table 1) and this structural change causes a loss of approximately 4-fold in intrinsic potency against the enzyme. Replacement of the benzoyl moiety in **24** with naphthalene-1-carbonyl gave compound **25**, which showed good inhibitory activity against FTase, in analogy with related piperazine-based FTIs.³⁷ The benzoyl compound **24** was also compared to its simple chloro-substituted analogues (see structures **26–28** in Table 3) and, in analogy with the chlorobenzyl derivatives in Table 2, the 3-chloro isomer **27** was found to be the most potent inhibitor of FTase, with an IC₅₀ value of 27 nM. It seemed likely that the isomeric 1-acylpyrrolidine series bound to FTase in an analogous fashion to the pyrrolidinone series but offered an advantage in terms of ease of synthesis. It was possible to rapidly screen different acyl substituents, and we hoped that, by focusing on polar heterocycles as replacements for the chlorophenyl moieties in compounds such as **27**, it would be possible to identify pyrrolidine-based FTIs that had reduced affinity for the I_{Kr} channel.

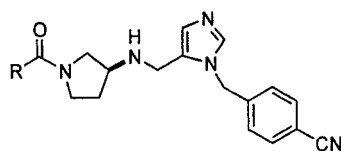
A subset of the compounds synthesized in this effort are illustrated in Table 3 (compounds **29–37**). A variety of heterocyclic acyl substituents was investigated, but the series of nicotinoyl derivatives in Table 3 serves to illustrate the general trends observed. As was expected, the more polar derivatives did possess reduced affinity for the ion channel. Compounds **31** and **32**, for example, had no measurable activity in the hERG assay, whereas the 3-chlorobenzoyl derivative **27** had a hERG inflection point of 5800 nM. Unfortunately, those compounds with the lowest affinity for the ion channel also exhibited unacceptably weak inhibition of FTase. For example, while the 2-methoxynicotinoyl derivative **33** showed very modest binding to the I_{Kr} channel (hERG IP = 21 000 nM), it was a poor enzyme inhibitor (FTase IC₅₀ = 150 nM). The related sulfide analogue **35** possessed slightly better activity against FTase (IC₅₀ = 83 nM), but homologation of this structure provided the ethyl sulfide **36**, which displayed an unexpected improvement in terms of inhibition of FTase (IC₅₀ = 4.8 nM). Substitution at other positions in this nicotinoyl system, to afford compounds such as the bromide **37**, failed to provide more potent FTIs than **36**. Indeed, Table 3 illustrates the profound effects of substitution at this

nicotinoyl 2-position on activity against FTase. The unsubstituted analogue **29** was a relatively poor inhibitor (IC₅₀ = 2000 nM), but addition of a methyl group improved the IC₅₀ value by 20-fold. Addition of polar groups at this position had little effect compared with **29** (see structures **31**, **32**, and **34**), but the addition of a thioethyl side chain to give **36** provided more than a 400-fold improvement in potency. This profound effect strongly suggested that the thioethyl side chain was making a specific interaction with some hydrophobic pocket on the enzyme, perhaps mimicking one of the amino acid side chains of the CaaX substrate. Modeling studies supported this idea, revealing low-energy conformations of **36** docked in the FTase active site in which the thioethyl group projected into the same pocket occupied by the chlorophenyl ring in **5h** (compare Figures 1 and 2). Moreover, when this conformation of **36** was overlaid with the crystallographically determined bound structure of the peptidomimetic FTI L-739,750,^{7a} the thioethyl moiety occupied the same space as the benzyl side chain in the peptidomimetic (Figure 2).

Compound **36** exhibited good cell potency (CRAFTI IC₅₀ = 6.2 nM) and excellent selectivity against GG-Tase-I (IC₅₀ = 5100 nM). Compared to the 3-chlorobenzoyl analogue **27**, the thioether **36** offered a significant improvement in potency against FTase. However, neither **36** nor any of the other acylpyrrolidines synthesized exhibited the excellent cell potency of compounds such as **5h**. We therefore sought other strategies to reduce the affinity of these aminopyrrolidine-based FTIs for the potassium channel.

One of the initially attractive features of the aminopyrrolidinone moiety in the context of FTIs was that the central backbone amino group may be regarded as a trivalent handle, allowing the exploration of SAR that is quite distinct from related inhibitors. This central nitrogen atom may be attached to a cyanobenzylimidazole group, which presumably interacts with the active site zinc ion, and to a potency-enhancing hydrophobe, such as the chlorophenyl in compound **5h**, via the pyrrolidine ring. This arrangement still leaves one position vacant on the central amine and, as such, permits facile exploration from this handle. Results from an investigation of such SAR in the context of the lead **5b** are shown in Table 4 (compounds **38–46**).

Initially, the amino group was derivatized with aliphatic groups such as *n*-butyl, which had only modest effects on the intrinsic enzyme potency (FTase IC₅₀ = 54 nM for **39**) but led to significant drops in the cell-based assay (CRAFTI IC₅₀ = 42 nM for **39** compared with 5.7 nM for **5b**). The availability of hydrophobic binding was probed by placing a phenyl group at various linker lengths from the amine (see compounds **40–43**). The optimal example appeared to be the phenylpropyl derivative **42**, but this possessed only a 2-fold enhanced IC₅₀ value vs FTase intrinsically and had markedly reduced cell potency (CRAFTI IC₅₀ = 74 nM). Reasoning that the increased lipophilicity of these structures relative to compound **5b** may be partly responsible for their poor performance in the cell-based assay, we investigated a number of relatively polar substituents to give compounds such as the amine **45** and the pyridine **46**. As Table 4 shows, these compounds fared

Table 3. 3-Aminopyrrolidine Inhibitors of FTase

Compound	R	FTase IC ₅₀ (nM) ^a	GGTase IC ₅₀ (nM) ^a	CRAFTI IC ₅₀ (nM) ^a	hERG IP (nM) ^a
24		110 (2)	24,000 (2)		
25		11 (2)	880 ± 200 (3)	330 (1)	
26		65 (2)	19,000 (2)		
27		27 (2)	11,000 (2)	67 (1)	5,800 ± 2,800 (3)
28		89 (1)	19,000 (1)	70 (1)	
29		2,000 (1)	> 50,000 (1)		
30		100 (2)	> 50,000 (1)	610 (1)	> 10,000 (1)
31		980 (2)	> 50,000 (1)		> 50,000 (1)
32		6,800 (1)	> 50,000 (1)		> 50,000 (1)
33		150 (1)	> 50,000 (1)		21,000 (1)
34		2,900 (1)	> 50,000 (1)		11,000 (1)
35		83 (2)	28,000 (2)	120 (1)	7,800 (2)
36		4.8 (2)	5,100 (2)	6.2 (2)	14,000 ± 9,900 (3)
37		43 (2)	41,000 (2)	49 (2)	6,000 (2)

^a Number of replicates used to determine IC₅₀ values shown in parentheses.

no better in terms of inhibitory potency either intrinsically or in cells. Indeed, the cell-based potency of amine **45** was particularly poor, which may be attributable to the basic character of the substituent.

At this point, we concluded that these substituents had little effect on inhibition of FTase: the intrinsic IC₅₀

values are all within 2-fold of the parent compound **5b**. One explanation for this behavior is that the additional side chains are not making significant contacts with the enzyme active site but are oriented toward the solvent. Indeed, this explanation seems to be consistent with the modeled structure of the ternary complex of **5h** bound

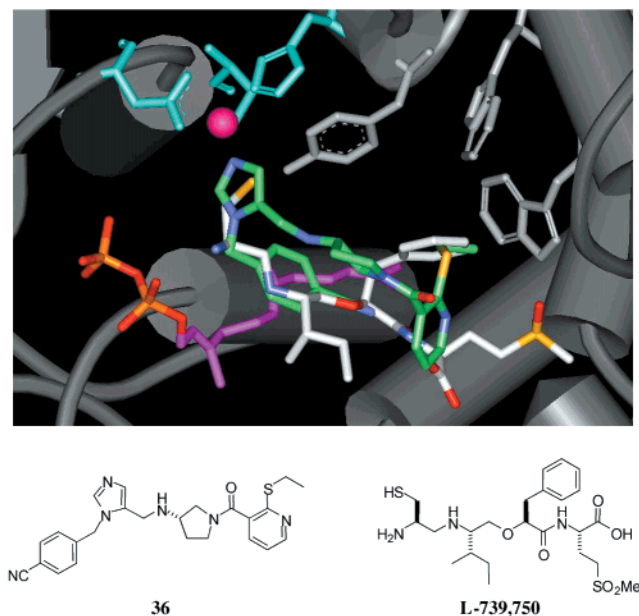


Figure 2. Docked structure of compound **36** (green) in the FTase active site overlaid with the bound conformation of the peptidomimetic FTI L-739,750^{7a} (white) as determined by X-ray crystallography.⁴⁴ Other details of the docking experiment and graphical representation are described in the Figure 1 legend.

to FTase, in which the amino group is oriented toward bulk solvent (see Figure 1). The analogues in Table 4 demonstrated generally good selectivity against GGTase-I and the data indicate that this enzyme is somewhat more sensitive to such substitutions than FTase. Compared with the parent structure **5b**, the substituents in some cases gave rise to more than 10-fold enhancements in the inhibitory activity against GGTase-I, and in other cases abolished all activity. Of greater concern was the observation that most of these tertiary amine analogues did not exhibit the same ratio of cell-based potency to intrinsic potency seen for compound **5b**, suggesting that this favorable behavior is related to the presence of the secondary amine functionality in compounds such as **5b** and **5h**. Nonetheless, the discovery of binding to the I_{Kr} channel by compounds such as **5h** prompted us to reexamine this kind of substitution pattern. We reasoned that an additional substituent on the amino group of **5h** should have a minor effect on its binding to FTase and that some moderately polar substituent might simultaneously maintain good cell penetration and also attenuate the affinity for the hERG channel.

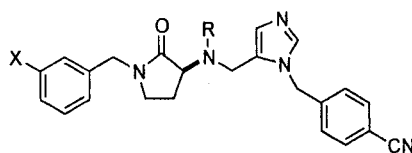
For comparison purposes, the phenylpropyl analogue of **5h** was synthesized (compound **47**) and, as expected, it was comparable to **5h** in terms of ability to inhibit FTase but was less effective in cells and possessed very high affinity for the I_{Kr} channel (hERG IP = 24 nM). A number of polar side chains were added to structure **5h** (compounds **48**–**54**), and it was found that while they caused minimal changes to the compound's intrinsic potency against FTase, the activity in cells ranged from excellent (CRAFTI IC₅₀ = 1.1 nM for compound **48**) to poor (CRAFTI IC₅₀ = 300 nM for compound **54**). It appeared that the best ratios of cell-based to intrinsic potency were obtained with moderately polar side chains such as the carbamate in **48**. Disappointingly,

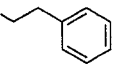
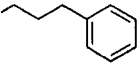
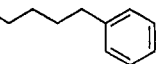
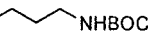
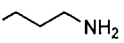
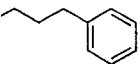
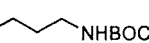
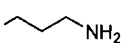
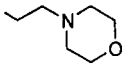
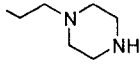
none of these analogues offered a significant advantage over the parent compound **5h** in terms of hERG activity (see Table 4).

Evaluation of the pharmacokinetic properties of **5h** in dogs revealed that the compound exhibited low plasma clearance (CL_p = 5.84 ± 0.12 mL/min/kg) but a half-life of only 1.07 ± 0.20 h due to a relatively low volume of distribution (Vd_{ss} = 0.45 ± 0.07 L/kg). Despite excellent bioavailability (F = 81 ± 16%), this profile was probably not suitable for oral dosing because, if such a short half-life were observed in humans, it would lead to significant peak to trough variations and possible prolongation of the QT_c interval at the peak plasma concentrations of drug. In contrast, the low rate of clearance would facilitate an intravenous dosing protocol. Therefore, a more accurate examination of the potency of **5h** seemed appropriate in order to establish if there was a suitable window between therapeutic plasma levels and potential proarrhythmic effects in vivo.

As described above, compound **5h** exhibited excellent potency in the cell-based radioligand displacement assay, with a CRAFTI IC₅₀ value that was some 4-fold lower than its intrinsic IC₅₀ for inhibition of FTase in vitro (see Table 2). The high cell potency of **5h** in CRAFTI translated from the radioligand binding assay into cell growth assays, and representative results are detailed in Table 5. As shown, compound **5h** inhibited the anchorage-independent growth of cultured H-*ras*-transformed Rat1 cells on poly(HEMA)-coated microtiter plates with an IC₅₀ value of 4.1 nM. This low nanomolar activity contrasted with the cytotoxic endpoint of the compound for Rat1 cells, which was determined to be greater than 100 μM by MTT staining. These data suggest that the FTI-mediated growth inhibition of the H-*ras*-transformed cells was at least partly due to inactivation of the mutant H-Ras protein. The inhibition of H- and K-*ras*-transformed Rat1 cell growth in soft agar by FTI **5h** was also studied. The compound proved to be extremely potent in this assay, inhibiting 90% of colony formation at 3–10 nM for the H-*ras* cell line and at 30 nM for the K-*ras* cell line, again showing activity at concentrations well below those that were observed to cause cytotoxicity (see Table 5). In contrast to the observations with H-*ras* transformed fibroblasts, the growth of H-*ras*-CVLL-transformed Rat1 cells, in which transformation is effected by an engineered Ras protein that is a selective substrate for GGTase-I, was much less sensitive to the FTI **5h** (IC₉₀ = 100–300 nM), consistent with the fact that the compound is a highly selective inhibitor of FTase. The fact that growth of this cell line was inhibited by **5h** at submicromolar concentrations indicates that a Ras-independent antiproliferative mechanism is operational in such fibroblasts.

The picture was more complex when a panel of human tumor cell lines was examined. Anchorage-independent growth was inhibited by **5h** for a variety of tumor types but, as has been observed for other FTIs,³⁸ there was no dependence on the mutational state of the *ras* gene. Thus, the growth of A549 cells, which contain a mutant K-*ras* gene, was inhibited to an almost identical extent to that of Colo-205 cells, which possess wild-type *ras* [poly(HEMA) IC₅₀ = 320 nM for A549 and 340 nM for Colo-205]. Similar results were observed for the human

Table 4. 3-Aminopyrrolidinone Inhibitors of FTase

Compound	X	R	FTase IC ₅₀ (nM) ^a	GGTase IC ₅₀ (nM) ^a	CRAFTI IC ₅₀ (nM) ^a	hERG IP (nM) ^a
38	H	n-Pr	59 ± 17 (4)		36 (1)	
39	H	n-Bu	54 ± 39 (5)		42 (1)	190 (1)
40	H		67 (2)	20,000 ± 1,700 (3)		
41	H		51 (2)	15,000 ± 3,400 (3)	460 (1)	
42	H		15 (2)	12,000 ± 2,200 (3)	74 (1)	
43	H		42 (1)	4,600 ± 890 (4)	310 (1)	
44	H		18 (2)	3,600 ± 710 (3)	65 (2)	
45	H		17 (1)	> 50,000 (1)	1,100 (1)	
46	H		52 (2)	> 50,000 (1)	110 (1)	870 (1)
47	Cl		2.5 (2)	6,500 (2)	12 (1)	24 (2)
48	Cl		1.3 (2)	2,700 (2)	1.1 (1)	110 (2)
49	Cl		7.5 (2)	> 50,000 (1)	150 (1)	480 (2)
52	Cl		6.0 (2)	12,000 (2)	3.3 (1)	190 (2)
54	Cl		6.1 (2)	> 50,000 (2)	300 (1)	1,100 (2)

^a Number of replicates used to determine IC₅₀ values shown in parentheses.

tumor cell lines LS180 (mutant *K-ras*) and MDA-MB-468 (wild-type *ras*) (see Table 5). In these human cell lines, the growth inhibition apparently did not result from inhibition of the prenylation of mutant Ras but from lack of farnesylation of some other protein(s). This result was not surprising, since it was known that in

cells K-Ras is geranylgeranylated by GGTase-I in the presence of a potent inhibitor of farnesyltransferase and that inhibition of K-Ras processing does not correlate with inhibition of cell growth.³⁹ Compound 5h, a highly selective FTI, could inhibit farnesylation of K-Ras, but the protein would still become prenylated and, presum-

Table 5. Anchorage-Independent Cell Growth Inhibition by Compound **5h**

poly(HEMA)		soft agar	
cell line	IC ₅₀ (nM) ^a	cell line	IC ₉₀ (nM) ^a
H- <i>ras</i>	4.1 (2)	H- <i>ras</i>	3–10 (2)
A549	320 ± 88	K- <i>ras</i>	30 (2)
Colo-205	340 ± 300 (4)	H- <i>ras</i> -CVLL	100–300 (2)
LS180	530 ± 250 (8)		
KB-31	530 ± 63 (4)		
MDA-MB-468	750 ± 490 (4)		
DLD1	1600 ± 300 (3)		
DuPro-1	>100000 (2)		

^a Number of replicates used to determine IC₅₀ values shown in parentheses. Standard deviations from the mean are shown for IC₅₀ values determined three or more times.

Table 6. Effects of Compound **5h** in the K-*RasB* Transgenic Mouse Model

dose ^a (mg/kg/day)	plasma level ^b (μM)	MGR ^c (mm ³ /day)		% unprocessed mDJ2 ^d
		primary tumor	total	
vehicle		17.3 ± 3.5	19.9 ± 3.7	13 ± 2
40	0.67 ± 0.10	-3.1 ± 1.7	-3.9 ± 1.8	47 ± 9
120	1.8 ± 0.3	-1.2 ± 2.0	-1.0 ± 2.1	79 ± 1

^a Compound dosed for 28 days subcutaneously in 50% aqueous DMSO using osmotic minipumps, 10 animals per dose group. ^b Plasma level of compound (±SEM) determined at termination of study using HPLC analysis. ^c Mean growth rate of tumor volume (±SEM) measured for both the primary tumor and also for the total tumor volume in the animal. ^d Percentage (±SEM) of mDJ2 protein in the mouse spleen determined to be unfarnesylated by a standard Western blot assay at the termination of the experiment.

ably, functional. The identity of the real target or targets of FTIs has been the subject of much research and discussion.³ A number of proteins, including RhoB⁴⁰ and CENP-E,⁴¹ have been postulated to be the relevant FTase substrate(s), but more work remains to be done. It was clear, in any case, that compound **5h** could inhibit the growth of a variety of artificially transformed cells and human tumor cell lines and a key question was whether this effect could be reproduced in vivo.

As an in vivo model of cancer, the K-*rasB* transgenic mouse model of cancer has a number of attractive features, notably that the mice are not immune-compromised and that the tumors occur and grow spontaneously in the animals, in contrast to the transplanted foreign tumor cells used in nude mouse experiments.³¹ We were interested in establishing what steady-state plasma levels would be required for full efficacy, so we examined the effects of **5h** in K-*rasB* transgenic mice with the compound being administered by subcutaneous infusion for 28 days. Table 6 summarizes the results of these experiments. As can be seen, at doses of 120 and 40 mg/kg/day, regression of both primary tumor and total tumor volume was noted. The regressions seen in these studies represented maximal responses for both doses, so it may be assumed that the 120 mg/kg/day regimen constitutes an excessive dose. The percentage of unprocessed mDJ2, a protein substrate for FTase, was quantitated using spleen tissue from the mice to give a measure of in vivo FTase inhibition, and the results confirmed the very high level of FTase inhibition in the 120 mg/kg/day dose group (79% unprocessed mDJ2) compared with the 40 mg/kg/day group (47% unprocessed mDJ2). The overdosing of FTI at the highest dose was also manifested in terms of gross toxicity in the mice in that 20% of the animals

died during the experiment. The lower dose of **5h** was significantly less toxic and resulted in no lethality. These experiments demonstrate that **5h** acts as an effective antitumor agent in a K-*ras* mouse model of cancer, despite the fact that the mutant K-Ras protein is presumably prenylated under the experimental conditions.

Conclusion

A series of 3-aminopyrrolidinone-based inhibitors of farnesyltransferase has been developed. Systematic modification of these structures led to the identification of **5h**, a highly potent, low molecular weight, non-thiol, non-peptide FTI that was efficacious both in cell culture and in animals. The compound was extremely potent in cell-based experiments, inhibiting the growth of a variety of transformed cells with submicromolar IC₅₀ values. While compound **5h** exhibited low plasma clearance and excellent oral bioavailability, its relatively short plasma half-life in conjunction with its effects on the QT_c interval in dogs made it unacceptable as a candidate for oral dosing. Although the window between plasma levels that showed full efficacy in the K-*rasB* transgenic mouse (0.67 μM) and those that caused 10% prolongation of the QT_c interval in dogs (2.5 μM) would potentially allow a successful intravenous dosing protocol, a variety of modifications have been explored in an attempt to improve this window to a degree that would permit oral dosing in a clinical setting. While binding to the I_{Kr} ion channel was significantly reduced in some cases, the modifications required were not consistent with maintaining the high levels of potency against FTase seen with compound **5h**. Nonetheless, the 3-aminopyrrolidinone core appeared to confer a very favorable ratio of cell-based potency to intrinsic potency, and this was due in part to the fact that compounds such as **5h** appeared to be relatively poor substrates for the P-glycoprotein pump. This property may help prevent chemoresistance in treated tumors and facilitate the effort to identify clinically useful chemotherapy agents.

Experimental Section

General Methods. Proton NMR spectra were run at 300 MHz on a Varian VXR-300 or at 400 MHz on a Varian Unity 400 or VXR-400 spectrometer, and chemical shifts are reported in parts per million (δ) downfield from tetramethylsilane as internal standard. Fast atom bombardment mass spectra were recorded on a VG-ZAB-HF spectrometer using glycerol as matrix. Electrospray mass spectra were recorded on a Micro-mass ZMD spectrometer. Elemental analyses were performed using a Perkin-Elmer 2400 model II elemental analyzer. Silica gel 60 (230–400 mesh) from EM Science was used for column chromatography, and analytical or preparative thin-layer chromatography was conducted using EM Science Kieselgel 60 F₂₅₄ plates. Thermoseparation HPLC equipment with a Vydac C18 reversed phase column was used for analytical or preparative HPLC. The elution used either a gradient of 95/5 to 0/100 A/B; A = H₂O–0.1% TFA, B = CH₃CN–0.1% TFA (method A), or a gradient of 95/5 to 5/95 A/B; A = H₂O–0.1% H₃PO₄, B = CH₃CN (method B). The enantiomeric purity of the final compounds was established by HPLC using either a Chiralpak AD or a Chiralcel OD column or by Mosher amide analysis. For reactions performed under anhydrous conditions, glassware was either oven- or flame-dried and the reaction was run under a positive pressure of argon. Tetrahydrofuran was freshly distilled from sodium/benzophenone; all other anhydrous solvents were used as purchased from Aldrich.

Except where noted, reagents were purchased from Aldrich and used without further purification. The reported yields are the actual isolated yields of purified material and are not optimized.

(S)-4-[5-[(2-Oxo-1-phenylpyrrolidin-3-ylamino)methyl]imidazol-1-ylmethyl]benzotrile Hydrochloride (5a). **(S)-2-(tert-Butoxycarbonylamino)-4-(methylmercapto)-N-phenylbutyramide (2a).** To (S)-N-(tert-butoxycarbonyl)-methionine (589 mg, 2.36 mmol) in dry CH₂Cl₂ (5 mL) under argon were added PYBOP (1.23 g, 2.36 mmol), aniline (196 μ L, 2.14 mmol), and N,N-diisopropylethylamine (655 μ L, 3.76 mmol). The reaction mixture was stirred for 1 h and then quenched with 10% citric acid (20 mL) and extracted with CH₂-Cl₂ (2 \times 20 mL). The combined organic extracts were dried over MgSO₄, filtered, and concentrated in vacuo. The crude product was purified by flash column chromatography on silica, eluting with hexane–15% ethyl acetate to yield the product as a white solid (690 mg, 99%): ¹H NMR (CDCl₃) δ 8.27 (1H, br s), 7.51 (2H, d, *J* = 8.4 Hz), 7.32 (2H, t, *J* = 7.8 Hz), 7.12 (1H, t, *J* = 7.1 Hz), 5.20 (1H, br d, *J* = 7.1 Hz), 4.40 (1H, m), 2.70–2.56 (2H, m), 2.20 (1H, m), 2.14 (3H, s), 2.02 (1H, m), 1.47 (9H, s); MS (FAB) *m/z* = 325 (M⁺ + H); HPLC purity = 99.1% (method A, 215 nm).

(S)-2-(tert-Butoxycarbonylamino)-4-(dimethylsulfonium)-N-phenylbutyramide Iodide. (S)-2-(tert-Butoxycarbonylamino)-4-(methylmercapto)-N-phenylbutyramide (2a) (680 mg, 2.10 mmol) was dissolved in iodomethane (10 mL, 160 mmol) and the solution was stirred under argon for 48 h. The iodomethane was removed by distillation under reduced pressure to give the sulfonium salt as a white solid of sufficient purity for use in the next step: ¹H NMR (CDCl₃) δ 9.77 (1H, br s), 7.81 (2H, d, *J* = 7.9 Hz), 7.29 (2H, t, *J* = 7.9 Hz), 7.10 (1H, t, *J* = 7.0 Hz), 6.11 (1H, d, *J* = 7.0 Hz), 4.79 (1H, m), 3.72 (1H, m), 3.49 (1H, m), 3.28 (3H, s), 3.04 (3H, s), 2.87 (1H, m), 2.13 (1H, m), 1.44 (9H, s); MS (FAB) *m/z* = 339 (M⁺).

(S)-3-(tert-Butoxycarbonylamino)-2-oxo-1-phenylpyrrolidine (3a). (S)-2-(tert-Butoxycarbonylamino)-4-(dimethylsulfonium)-N-phenylbutyramide iodide (970 mg, 2.1 mmol) was stirred in dry THF (40 mL), under argon, at 0 °C, and lithium bis(trimethylsilyl)amide (1.0 M in THF, 2.1 mL, 2.1 mmol) was added dropwise. The reaction mixture was stirred at 0 °C for 2 h and then quenched with saturated aqueous NH₄Cl (5 mL), and most of the THF was removed under reduced pressure. The residual solution was partitioned between saturated aqueous NaHCO₃ (10 mL) and CH₂Cl₂ (20 mL). The aqueous layer was extracted further with CH₂Cl₂ (2 \times 20 mL), and the combined organic extracts were dried over MgSO₄, filtered, and concentrated in vacuo. The crude product was purified by flash column chromatography on silica, eluting with hexane–20% ethyl acetate to yield the pyrrolidinone as a white solid (560 mg, 97%): ¹H NMR (CDCl₃) δ 7.64 (2H, dd, *J* = 8.8, 1.0 Hz), 7.39 (2H, dd, *J* = 8.5, 7.6 Hz), 7.18 (1H, tt, *J* = 7.3, 1.0 Hz), 5.23 (1H, br s), 4.35 (1H, m), 3.87–3.75 (2H, m), 2.80 (1H, m), 2.00 (1H, qn, *J* = 10.7 Hz), 1.48 (9H, s); MS (FAB) *m/z* = 277 (M⁺ + H); HPLC purity = 98.5% (method A, 215 nm); ee = 96.4%.

(S)-3-Amino-2-oxo-1-phenylpyrrolidine Hydrochloride (4a). A solution of (S)-3-(tert-butoxycarbonylamino)-2-oxo-1-phenylpyrrolidine (3a) (490 mg, 1.8 mmol) in EtOAc (40 mL) at 0 °C was saturated with HCl(g). After 15 min, the mixture was concentrated in vacuo to yield the amine hydrochloride as a pale solid (380 mg, 99%): ¹H NMR (CD₃OD) δ 7.67 (2H, dd, *J* = 8.8, 0.9 Hz), 7.41 (2H, dd, *J* = 8.4, 7.7 Hz), 7.23 (1H, t, *J* = 7.4 Hz), 4.26 (1H, dd, *J* = 10.9, 8.7 Hz), 3.99 (1H, td, *J* = 9.9, 6.2 Hz), 3.96 (1H, m), 2.69 (1H, m), 2.16 (1H, m); MS (FAB) *m/z* = 177 (M⁺ + H); HPLC purity = 100.0% (method A, 215 nm).

(S)-4-[5-[(2-Oxo-1-phenylpyrrolidin-3-ylamino)methyl]imidazol-1-ylmethyl]benzotrile Hydrochloride (5a). (S)-3-Amino-2-oxo-1-phenylpyrrolidine (4a) (100 mg, 0.57 mmol), 1-(4-cyanobenzyl)-5-imidazolecarboxaldehyde¹¹ (132 mg, 0.62 mmol), and acetic acid (98 μ L, 1.71 mmol) were stirred in MeOH (2 mL) for 1 h, then NaCNBH₃ (47 mg, 0.74 mmol) was added. Stirring was continued for 1 h, then the reaction was

quenched with saturated aqueous NaHCO₃ (2 mL) and most of the MeOH was removed under reduced pressure. The residual solution was partitioned between saturated aqueous NaHCO₃ (3 mL) and CH₂Cl₂ (5 mL). The aqueous layer was extracted further with CH₂Cl₂ (2 \times 5 mL). The combined organic extracts were dried over MgSO₄, filtered, and concentrated in vacuo. The crude product was purified by flash column chromatography on silica, eluting with CH₂Cl₂–2% MeOH–0.2% NH₄OH, to yield the desired product, which was treated with aqueous HCl in acetonitrile to afford the hydrochloride salt as a white solid (215 mg, 85%): ¹H NMR (CD₃-OD) δ 9.15 (1H, s), 7.95 (1H, d, *J* = 1.1 Hz), 7.82 (2H, d, *J* = 8.6 Hz), 7.67 (2H, d, *J* = 8.8 Hz), 7.57 (2H, d, *J* = 8.6 Hz), 7.43 (2H, dd, *J* = 8.6, 7.5 Hz), 7.26 (1H, t, *J* = 7.5 Hz), 5.83 (2H, s), 4.81 (1H, d, *J* = 15.0 Hz), 4.53 (1H, d, *J* = 15.0 Hz), 4.44 (1H, dd, *J* = 10.7, 8.7 Hz), 4.00–3.95 (2H, m), 2.75 (1H, m), 2.31 (1H, m); MS (FAB) *m/z* = 372 (M⁺ + H); HPLC purity = 97.3% (method A, 215 nm); ee = 93.9%. Anal. (C₂₂H₂₁N₅O·1.7HCl·1.7H₂O·0.2EtOAc) C, H, N.

(R)-4-[5-[2-(1-Benzyl-2-oxopyrrolidin-3-ylamino)ethyl]imidazol-1-ylmethyl]benzotrile Hydrochloride (12b). **4-[5-(2-Hydroxyethyl)imidazol-1-ylmethyl]benzotrile.** To a stirred solution of methyl [1-(4-cyanobenzyl)-1H-imidazol-5-yl]acetate¹⁶ (1.09 g, 4.28 mmol) in methanol at 0 °C was added sodium borohydride (0.96 g, 25.4 mmol) in one portion. After 3 h, saturated aqueous NH₄Cl (20 mL) was added, followed by saturated aqueous NaHCO₃ (20 mL), and the mixture was extracted with EtOAc (3 \times 75 mL). The combined organic extracts were dried over MgSO₄, filtered, and concentrated in vacuo. The crude product was purified by flash column chromatography on silica, eluting with CH₂Cl₂–5% MeOH, to yield the desired product as a white solid (490 mg, 50%): ¹H NMR (CDCl₃) δ 7.64 (2H, d, *J* = 8.4 Hz), 7.50 (1H, s), 7.12 (2H, d, *J* = 8.6 Hz), 6.95 (1H, d, *J* = 0.7 Hz), 5.23 (2H, s), 3.79 (2H, t, *J* = 6.4 Hz), 2.66 (2H, td, *J* = 6.4, 0.9 Hz), 1.94 (1H, br s); MS (FAB) *m/z* = 228 (M⁺ + H).

Methanesulfonic Acid 2-[1-(4-cyanobenzyl)-1H-imidazol-5-yl]ethyl Ester (10). A solution of 4-[5-(2-hydroxyethyl)-imidazol-1-ylmethyl]-benzotrile (250 mg, 1.10 mmol) in dry CH₂Cl₂ (35 mL) at 0 °C, under argon, was treated with N,N-diisopropylethylamine (233 μ L, 1.34 mmol), followed by methanesulfonyl chloride (103 μ L, 1.33 mmol). The reaction mixture was stirred at 0 °C for 3 h and then quenched with saturated aqueous NaHCO₃ (25 mL) and extracted with CH₂Cl₂ (3 \times 15 mL). The combined organic extracts were dried over MgSO₄, filtered, and concentrated in vacuo to give the mesylate as a thick yellow oil, which was used crude for the next reaction: ¹H NMR (CDCl₃) δ 7.66 (2H, d, *J* = 8.4 Hz), 7.56 (1H, s), 7.14 (2H, d, *J* = 8.4 Hz), 7.01 (1H, d, *J* = 0.5 Hz), 5.21 (2H, s), 4.31 (2H, t, *J* = 6.7 Hz), 2.95 (3H, s), 2.87 (2H, td, *J* = 6.7, 0.7 Hz).

(R)-4-[5-[2-(1-Benzyl-2-oxopyrrolidin-3-ylamino)ethyl]imidazol-1-ylmethyl]benzotrile Hydrochloride (12b). Methanesulfonic acid 2-[1-(4-cyanobenzyl)-1H-imidazol-5-yl]ethyl ester (10) (173 mg, 0.57 mmol), (R)-3-amino-1-benzyl-2-oxopyrrolidine (synthesized in analogy with compound 4a) (80 mg, 0.42 mmol), sodium iodide (126 mg, 0.84 mmol), and N,N-diisopropylethylamine (110 μ L, 0.63 mmol) were combined in dry, degassed DMF (2 mL) and heated to 50 °C, under argon, for 18 h. The reaction was quenched with saturated aqueous NaHCO₃ (2 mL) and then concentrated under reduced pressure. The residue was partitioned between saturated aqueous NaHCO₃ (5 mL) and CH₂Cl₂ (5 mL). The aqueous layer was extracted further with CH₂Cl₂ (3 \times 5 mL). The combined organic extracts were dried over MgSO₄, filtered, and concentrated in vacuo. The crude product was partially purified by flash column chromatography on silica, eluting with a gradient of CHCl₃–3% to 4% MeOH–0.3% to 0.4% NH₄OH and then further purified by preparative TLC, eluting with CHCl₃–6% MeOH–0.6% NH₄OH, to yield the desired product, which was converted to the hydrochloride salt by treatment with aqueous HCl in acetonitrile (43 mg, 22%): ¹H NMR (CD₃OD) δ 9.10 (1H, d, *J* = 1.5 Hz), 7.83 (2H, d, *J* = 8.6 Hz), 7.68 (1H, d, *J* = 1.3 Hz), 7.51 (2H, d, *J* = 8.4 Hz), 7.38–7.28 (5H, m), 5.66 (2H, s), 4.53 (1H, d, *J* = 14.8 Hz), 4.48 (1H, d, *J* = 14.6 Hz), 4.24

(1H, dd, $J = 10.2, 8.9$ Hz), 3.65 (1H, m), 3.47–3.35 (3H, m), 3.09 (2H, dd, $J = 8.4, 7.3$ Hz), 2.55 (1H, m), 2.09 (1H, m); MS (FAB) $m/z = 400$ ($M^+ + H$); HPLC purity = 90.2% (method A, 215 nm); ee = 90.4%. Anal. ($C_{24}H_{25}N_5O \cdot 2.5HCl \cdot 0.65CH_3CN \cdot 0.85C_6H_5CH_3$) C, H, N.

(S)-4-(5-([2-Oxo-1-(2-pyridyl)pyrrolidin-3-ylamino]methyl)imidazol-1-ylmethyl)benzotrile Hydrochloride (16). (S)-3-Amino-2-oxo-1-(2-pyridyl)pyrrolidine dihydrochloride. A solution of (S)-3-(*tert*-butoxycarbonylamino)-2-oxo-1-(2-pyridyl)pyrrolidine¹⁷ (65 mg, 0.23 mmol) in EtOAc (5 mL) at 0 °C was saturated with HCl(g). After 15 min, the mixture was concentrated in vacuo to yield the amine hydrochloride as a white solid (59 mg, 100%): ¹H NMR (CD_3OD) δ 8.43 (1H, ddd, $J = 5.1, 1.9, 0.8$ Hz), 8.29 (1H, dt, $J = 8.6, 0.9$ Hz), 7.96 (1H, ddd, $J = 8.5, 7.4, 1.8$ Hz), 7.29 (1H, ddd, $J = 7.3, 5.1, 1.1$ Hz), 4.37 (1H, dd, $J = 11.0, 8.8$ Hz), 4.33 (1H, ddd, $J = 10.5, 9.2, 1.1$ Hz), 3.82 (1H, td, $J = 10.5, 6.7$ Hz), 2.70 (1H, m), 2.16 (1H, m); ee > 99%, as determined by synthesis of the corresponding Mosher amide diastereomers and ¹H NMR analysis.¹⁷

(S)-4-(5-([2-Oxo-1-(2-pyridyl)pyrrolidin-3-ylamino]methyl)imidazol-1-ylmethyl)benzotrile Hydrochloride (16). (S)-3-Amino-2-oxo-1-(2-pyridyl)pyrrolidine dihydrochloride (58 mg, 0.23 mmol) and 1-(4-cyanobenzyl)-5-imidazolecarboxaldehyde¹¹ (56 mg, 0.27 mmol) were combined in MeOH (1 mL), and the solution was adjusted to ca. pH \approx 5 (as judged by wetted pH indicator paper) by addition of *N,N*-diisopropylethylamine and then stirred at ambient temperature for 30 min. NaCNBH₃ (17 mg, 0.27 mmol) was added and the solution was adjusted to pH \approx 5 by addition of acetic acid. Stirring was continued for 18 h, then the reaction was quenched with a few drops of 10% aqueous citric acid, and the mixture was stirred for 10 min. Saturated aqueous Na₂CO₃ (5 mL) was added and the mixture was extracted with CH₂Cl₂ (4 \times 20 mL) and then EtOAc (2 \times 20 mL). The combined organic extracts were dried over Na₂SO₄, filtered, and concentrated in vacuo. The crude material was purified by flash column chromatography on silica, eluting with a gradient of CH₂Cl₂-1% to 6% MeOH-0.25% NH₄OH, to yield the desired product: ¹H NMR ($CDCl_3$) δ 8.38–8.34 (2H, m), 7.71 (1H, ddd, $J = 8.6, 7.3, 1.8$ Hz), 7.62 (2H, d, $J = 8.2$ Hz), 7.54 (1H, d, $J = 0.9$ Hz), 7.19 (2H, d, $J = 8.6$ Hz), 7.09–7.04 (2H, m), 5.44 (1H, d, $J = 16.5$ Hz), 5.39 (1H, d, $J = 16.5$ Hz), 4.16 (1H, ddd, $J = 11.2, 9.0, 1.9$ Hz), 3.86 (1H, d, $J = 13.7$ Hz), 3.78 (1H, ddd, $J = 11.2, 9.9, 6.8$ Hz), 3.72 (1H, d, $J = 13.7$ Hz), 3.58 (1H, dd, $J = 10.2, 8.0$ Hz), 2.27 (1H, m), 1.70 (1H, m). The free base was treated with HCl in EtOAc to afford the hydrochloride salt as a white solid (95 mg, 92%); MS (FAB) $m/z = 373$ ($M^+ + H$); HPLC purity = 98.0% (method B, 215 nm). Anal. ($C_{21}H_{20}N_6O \cdot 2.5HCl \cdot 0.4H_2O \cdot 0.1EtOAc$) C, H, N.

(S)-4-(5-([1-(Naphthalene-1-carbonyl)pyrrolidin-3-ylamino]methyl)imidazol-1-ylmethyl)benzotrile Hydrochloride (25). (S)-1-(*tert*-Butoxycarbonyl)-3-(trifluoroacetamido)pyrrolidine. To a stirred solution of (S)-3-(trifluoroacetamido)pyrrolidine hydrochloride (20) (TCI) (2.08 g, 9.5 mmol) and *N,N*-diisopropylethylamine (1.82 mL, 10.5 mmol) in CH₂Cl₂ (25 mL) was added di-*tert*-butyl dicarbonate (2.08 g, 9.5 mmol) in CH₂Cl₂ (25 mL). The reaction mixture was stirred at ambient temperature for 2 h and then partitioned between saturated aqueous Na₂CO₃ (30 mL) and CH₂-Cl₂ (50 mL). The aqueous layer was extracted further with CH₂Cl₂ (50 mL). The combined organic extracts were dried over Na₂SO₄, filtered, and concentrated in vacuo to give a crude product that was sufficiently pure for use in the next step: ¹H NMR ($CDCl_3$) δ 6.46 (1H, br d), 4.50 (1H, m), 3.67 (1H, dd, $J = 11.7, 6.2$ Hz), 3.56–3.22 (3H, m), 2.23 (1H, m), 1.95 (1H, br s), 1.47 (9H, s).

(S)-3-Amino-1-(*tert*-butoxycarbonyl)pyrrolidine (21). To a stirred solution of (S)-1-(*tert*-butoxycarbonyl)-3-(trifluoroacetamido)pyrrolidine (2.80 g, 9.5 mmol) in THF (80 mL) and H₂O (10 mL) was added 1.0 N aqueous lithium hydroxide (10.5 mL, 10.5 mmol), and the resulting mixture was stirred at ambient temperature for 18 h and then adjusted to pH 7 with 1.0 N aqueous HCl and concentrated to dryness in vacuo

to give the titled compound, which was of sufficient purity for use in the next step: ¹H NMR (CD_3OD) δ 3.76 (1H, m), 3.62 (1H, m), 3.55–3.38 (2H, m), 3.29 (1H, m), 2.24 (1H, m), 1.93 (1H, m), 1.46 (9H, s).

(S)-3-([1-(4-Cyanobenzyl)-1H-imidazol-5-ylmethyl]amino)pyrrolidine-1-carboxylic Acid *tert*-Butyl Ester (22). (S)-3-Amino-1-(*tert*-butoxycarbonyl)pyrrolidine (1.18 g, 6.34 mmol) (21), 1-(4-cyanobenzyl)-5-imidazolecarboxaldehyde¹¹ (1.41 g, 6.68 mmol), and acetic acid (0.363 mL, 6.34 mmol) were stirred in MeOH (35 mL) for 30 min, then NaCNBH₃ (0.44 g, 7.00 mmol) was added. Stirring was continued for 18 h, then the reaction was quenched with 10% aqueous citric acid (5 mL), followed by saturated aqueous Na₂CO₃ (50 mL), and the mixture was extracted with CH₂Cl₂ (2 \times 100 mL). The combined organic extracts were dried over Na₂SO₄, filtered, and concentrated in vacuo. The crude product was purified by flash column chromatography on silica, eluting with a gradient of CH₂Cl₂-1% to 7% MeOH-0.5% NH₄OH, to yield the desired product as a white solid (1.96 g, 81% over 3 steps): ¹H NMR ($CDCl_3$) δ 7.64 (2H, d, $J = 8.4$ Hz), 7.52 (1H, s), 7.16 (2H, d, $J = 7.9$ Hz), 6.99 (1H, s), 5.34 (2H, m), 3.63–2.94 (7H, m), 1.97 (1H, m), 1.59 (1H, m), 1.46 (9H, s).

(S)-3-([1-(4-Cyanobenzyl)-1H-imidazol-5-ylmethyl]amino)pyrrolidine Hydrochloride (23). A solution of (S)-3-([1-(4-cyanobenzyl)-1H-imidazol-5-ylmethyl]amino)pyrrolidine-1-carboxylic acid *tert*-butyl ester (22) (1.92 g, 5.03 mmol) in EtOAc (100 mL) at 0 °C was saturated with HCl(g). After 15 min, the mixture was concentrated in vacuo to yield the amine hydrochloride as a white solid (1.97 g, 100%): ¹H NMR (CD_3OD) δ 9.02 (1H, d, $J = 1.3$ Hz), 8.01 (1H, s), 7.84 (2H, d, $J = 8.6$ Hz), 7.58 (2H, d, $J = 8.2$ Hz), 5.83 (2H, s), 4.42 (2H, s), 4.22 (1H, m), 3.76–3.65 (3H, m), 3.42 (1H, dt, $J = 11.8, 7.7$ Hz), 2.55 (1H, m), 2.41 (1H, m).

(S)-4-(5-([1-(Naphthalene-1-carbonyl)pyrrolidin-3-ylamino]methyl)imidazol-1-ylmethyl)benzotrile Hydrochloride (25). (S)-3-([1-(4-Cyanobenzyl)-1H-imidazol-5-ylmethyl]amino)pyrrolidine (23) (40 mg, 0.143 mmol), 1-naphthoic acid (27 mg, 0.157 mmol), EDC (30 mg, 0.157 mmol), 1-hydroxybenzotriazole hydrate (24 mg, 0.157 mmol), and *N,N*-diisopropylethylamine (27 μ L, 0.157 mmol) were combined in DMF (0.5 mL), and the mixture was stirred at ambient temperature for 18 h. The solvent was removed under reduced pressure and the residue was partitioned between 10% aqueous citric acid (1 mL) and CHCl₃ (2 mL). The organic layer was discarded, and the aqueous layer was basified by addition of saturated aqueous Na₂CO₃ (1.4 mL) and then extracted with CHCl₃ (2 \times 2 mL). The combined organic extracts were dried over MgSO₄, filtered, and concentrated in vacuo. The crude product was purified by flash column chromatography on silica, eluting with CH₂Cl₂-3% MeOH-0.3% NH₄OH to yield the titled product, which was converted to the hydrochloride salt by treatment with aqueous HCl in acetonitrile: ¹H NMR (CD_3OD) δ 9.06 (1H, rotamer A, d, $J = 1.3$ Hz), 9.00 (1H, rotamer B, d, $J = 1.3$ Hz), 8.02–7.85 (4H, rotamers A and B, m), 7.85 (2H, rotamer A, d, $J = 8.4$ Hz), 7.73 (2H, rotamer B, d, $J = 8.2$ Hz), 7.62–7.54 (6H, rotamer A and 4H, rotamer B, m), 7.42 (2H, rotamer B, d, $J = 8.0$ Hz), 5.83 (2H, rotamer A, s), 5.67 (2H, rotamer B, s), 4.37–4.00 (4H, rotamers A and B, m), 3.91–3.84 (1H, rotamer A, m), 3.69–3.65 (1H, rotamer B, m), 3.56–3.27 (2H, rotamers A and B, m), 2.61–2.25 (2H, rotamers A and B, m). The free base was treated with HCl in EtOAc to afford the hydrochloride salt as a pale solid: MS (electrospray) $m/z = 436$ ($M^+ + H$); HPLC purity = 99.5% (method B, 215 nm). Anal. ($C_{27}H_{25}N_5O \cdot 2.4HCl \cdot 2.3H_2O$) C, H, N.

(S)-4-(5-([1-(Benzyl-2-oxopyrrolidin-3-yl)(3-*tert*-butoxycarbonylamino)propyl]amino)methyl)imidazol-1-ylmethyl)benzotrile (44). (S)-4-(5-([1-(Benzyl-2-oxopyrrolidin-3-ylamino)methyl]imidazol-1-ylmethyl)benzotrile (5b) (90 mg, 0.23 mmol), 3-(*tert*-butoxycarbonylamino)propionaldehyde⁴² (81 mg, 0.47 mmol), and acetic acid (27 μ L, 0.47 mmol) were stirred in MeOH (1 mL) for 1 h, then NaCNBH₃ (18 mg, 0.29 mmol) was added. Stirring was continued for 18 h, then most of the MeOH was removed under reduced pressure. The residue was partitioned between saturated

aqueous NaHCO₃ (3 mL) and CH₂Cl₂ (5 mL). The aqueous layer was extracted further with CH₂Cl₂ (2 × 5 mL). The combined organic extracts were dried over MgSO₄, filtered, and concentrated in vacuo. The crude product was purified by flash column chromatography on silica, eluting with CH₂Cl₂-2% MeOH-0.2% NH₄OH, to yield the desired product as a white solid (92 mg, 73%): ¹H NMR (CD₃OD) δ 7.76 (1H, d, *J* = 0.9 Hz), 7.69 (2H, d, *J* = 8.4 Hz), 7.42-7.34 (5H, m), 7.17 (2H, d, *J* = 8.2 Hz), 7.00 (1H, s), 6.50 (1H, br m), 5.71 (1H, d, *J* = 16.7 Hz), 5.55 (1H, d, *J* = 16.7 Hz), 4.50 (1H, d, *J* = 14.8 Hz), 4.31 (1H, d, *J* = 14.7 Hz), 3.72 (1H, t, *J* = 9.2 Hz), 3.63 (1H, d, *J* = 14.1 Hz), 3.58 (2H, t, *J* = 6.4 Hz), 3.54 (1H, d, *J* = 14.1 Hz), 3.22-3.15 (2H, m), 2.54 (1H, m), 2.43 (1H, m), 2.04 (1H, m), 1.92 (1H, m), 1.67 (2H, m), 1.43 (9H, s). The free base was treated with AcOH to afford the acetate salt as a gummy solid: MS (FAB) *m/z* = 543 (M⁺ + H); HPLC purity = 98.3% (method B, 215 nm). Anal. (C₃₁H₃₈N₆O₃·0.95AcOH·1.2H₂O) C, H, N.

(S)-4-(5-((3-Aminopropyl)(1-benzyl-2-oxopyrrolidin-3-yl)amino)methyl)imidazol-1-ylmethyl)benzotrile Hydrochloride (45). A solution (S)-4-(5-((1-benzyl-2-oxopyrrolidin-3-yl)-(3-*tert*-butoxycarbonylamino)propyl)amino)methyl)imidazol-1-ylmethyl)benzotrile (44) (625 mg, 1.15 mmol) in EtOAc (25 mL) at 0 °C was saturated with HCl(g). After 15 min, the mixture was concentrated in vacuo to yield the amine hydrochloride as a white solid (642 mg, 100%): ¹H NMR (CD₃OD) δ 9.05 (1H, d, *J* = 1.5 Hz), 7.79 (2H, d, *J* = 8.4 Hz), 7.75 (1H, s), 7.49 (2H, d, *J* = 8.4 Hz), 7.36-7.27 (3H, m), 7.21 (2H, d, *J* = 8.1 Hz), 5.82 (1H, d, *J* = 16.3 Hz), 5.74 (1H, d, *J* = 16.1 Hz), 4.49 (1H, d, *J* = 14.8 Hz), 4.43 (1H, d, *J* = 14.7 Hz), 3.95-3.78 (3H, m), 3.23 (2H, m), 2.97 (2H, t, *J* = 6.4 Hz), 2.77-2.60 (2H, m), 2.13-1.75 (4H, m); MS (FAB) *m/z* = 443 (M⁺ + H); HPLC purity = 100% (method B, 215 nm). Anal. (C₂₆H₃₀N₆O·2.5HCl·1.45H₂O) C, H, N.

(S)-4-[5-((1-(3-Chlorobenzyl)-2-oxopyrrolidin-3-yl)-(2-morpholin-4-ylethyl)amino)methyl)imidazol-1-ylmethyl)benzotrile Hydrochloride (52). **(S)-4-(5-((2-*tert*-Butyldimethylsilyloxyethyl)[1-(3-chlorobenzyl)-2-oxopyrrolidin-3-yl]amino)methyl)imidazol-1-ylmethyl)benzotrile.** A solution of amine 5h (203 mg, 0.48 mmol), 2-*tert*-butyldimethylsilyloxyethanal¹⁹ (126 mg, 0.73 mmol), and AcOH (83 μL, 1.45 mmol) in MeOH (2 mL) was stirred at ambient temperature for 30 min. NaCNBH₃ (61 mg, 0.0967 mmol) was added in one portion. After 15 h, the reaction was partitioned between saturated aqueous NaHCO₃ and CH₂Cl₂ and extracted with CH₂Cl₂ (3 × 50 mL). The organic extracts were combined, dried with Na₂SO₄, filtered, and concentrated in vacuo. The crude product was purified by flash column chromatography on silica, eluting with a gradient of CH₂Cl₂-1% to 3% MeOH-0.1% to 0.3% NH₄OH, to yield the titled product (213 mg, 76%): ¹H NMR (CDCl₃) δ 7.62 (2H, d, *J* = 8.2 Hz), 7.55 (1H, s), 7.29-7.23 (4H, m), 7.17 (1H, s), 7.06 (1H, m), 7.03 (1H, s), 5.65 (1H, d, *J* = 16.5 Hz), 5.57 (1H, d, *J* = 16.7 Hz), 4.44 (1H, d, *J* = 14.8 Hz), 4.35 (1H, d, *J* = 14.7 Hz), 3.79 (1H, m), 3.78 (1H, d, *J* = 9.2 Hz), 3.66 (1H, d, *J* = 13.7 Hz), 3.47 (2H, m), 3.14 (2H, m), 2.68 (1H, dt, *J* = 13.7, 5.5 Hz), 2.52 (1H, dt, *J* = 13.7, 6.6 Hz), 2.07 (1H, m), 1.91 (1H, m), 1.27 (9H, s), 0.86 (6H, s).

(S)-4-[5-((1-(3-Chlorobenzyl)-2-oxopyrrolidin-3-yl)-(2-hydroxyethyl)amino)methyl)imidazol-1-ylmethyl)benzotrile (50). To a stirred solution of (S)-4-(5-((2-*tert*-butyldimethylsilyloxyethyl)[1-(3-chlorobenzyl)-2-oxopyrrolidin-3-yl]amino)methyl)imidazol-1-ylmethyl)benzotrile (175 mg, 0.303 mmol) in THF (5 mL) was added TBAF (0.46 mL of a 1 M solution in THF, 0.46 mmol). After 10 min, the reaction was partitioned between H₂O and CH₂Cl₂ and extracted with CH₂Cl₂ (3 × 30 mL). The organic extracts were combined, dried with Na₂SO₄, filtered, and concentrated in vacuo. The crude product was purified by flash column chromatography on silica, eluting with a gradient of CH₂Cl₂-1% to 6% MeOH-0.1% to 0.6% NH₄OH, to yield the titled product (140 mg, 100%): ¹H NMR (CDCl₃) δ 7.63 (2H, d, *J* = 8.4 Hz), 7.58 (1H, s), 7.29-25 (3H, m), 7.25 (1H, s), 7.18 (1H, s), 7.07 (1H, m), 7.02 (1H, s), 5.70 (1H, d, *J* = 16.8 Hz), 5.43 (1H, d, *J* = 16.7 Hz), 4.44 (1H, d, *J* = 14.8 Hz), 4.86 (1H, d, *J* = 14.7 Hz), 3.98 (1H, br s), 3.63

(1H, d, *J* = 13.9 Hz), 3.61 (1H, dd, *J* = 8.4, 1.7 Hz), 3.56 (1H, d, *J* = 13.7 Hz), 3.42 (1H, m), 3.36 (1H, ddd, *J* = 11.5, 8.5, 3.1 Hz), 3.24-3.11 (2H, m), 2.66 (1H, m), 2.55 (1H, dt, *J* = 14.1, 3.8 Hz), 2.10 (1H, m), 1.84 (1H, m).

(S)-2-[[1-(3-Chlorobenzyl)-2-oxopyrrolidin-3-yl][3-(4-cyanobenzyl)imidazol-4-ylmethyl]amino]ethanal (51). To a solution of oxalyl chloride (35 μL, 0.39 mmol) in anhydrous CH₂Cl₂ (2 mL) at -78 °C was added dimethyl sulfoxide (35 μL, 0.78 mmol) over 5 min. After stirring for 10 min, a solution of alcohol 50 (140 mg, 0.303 mmol) in CH₂Cl₂ (2 mL) was added over 2 min. The resulting mixture was stirred at -78 °C for 15 min, then triethylamine (210 μL, 1.51 mmol) was added, and the reaction mixture was allowed to warm to ambient temperature over 1 h, after which saturated aqueous NH₄Cl (5 mL) was added. The mixture was poured into saturated aqueous NaHCO₃ (20 mL) and extracted with CH₂Cl₂ (3 × 50 mL). The combined organic extracts were dried over Na₂SO₄, filtered, and concentrated in vacuo to provide the crude product in sufficient purity for use in the next step: ¹H NMR (CDCl₃) δ 9.40 (1H, s), 7.61 (2H, d, *J* = 8.4 Hz), 7.56 (1H, s), 7.28-7.26 (4H, m), 7.24 (1H, s), 7.05 (1H, m), 7.03 (1H, s), 5.68 (1H, d, *J* = 16.7 Hz), 5.58 (1H, d, *J* = 16.7 Hz), 4.41 (1H, d, *J* = 14.7 Hz), 4.36 (1H, d, *J* = 14.8 Hz), 3.79 (1H, d, *J* = 13.7 Hz), 3.73 (1H, d, *J* = 13.7 Hz), 3.67 (1H, t, *J* = 9.4 Hz), 3.49 (1H, d, *J* = 18.5 Hz), 3.29 (1H, dd, *J* = 18.4, 0.8 Hz), 3.20-3.08 (2H, m), 2.06 (1H, m), 1.81 (1H, m).

(S)-4-(5-[[1-(3-Chlorobenzyl)-2-oxopyrrolidin-3-yl]-(2-morpholin-4-ylethyl)amino)methyl]imidazol-1-ylmethyl)benzotrile Hydrochloride (52). A solution of aldehyde 51 (46 mg, 0.10 mmol), morpholine (10 μL, 0.12 mmol), and AcOH (17 μL, 0.30 mmol) in MeOH (2 mL) was stirred at ambient temperature for 30 min. NaCNBH₃ (13 mg, 0.20 mmol) was added and the reaction mixture was stirred for 48 h and then partitioned between saturated aqueous NaHCO₃ (10 mL) and CH₂Cl₂ (20 mL). The aqueous layer was extracted further with CH₂Cl₂ (2 × 20 mL), and the organic extracts were combined, dried with Na₂SO₄, filtered, and concentrated in vacuo. The crude product was purified via preparative HPLC (method A), and the product-containing fractions were lyophilized. The resulting trifluoroacetate salt was free-based and treated with HCl in EtOAc to afford the titled product (13 mg, 25%): ¹H NMR (CD₃OD) δ 9.04 (1H, s), 7.81 (2H, d, *J* = 8.1 Hz), 7.74 (1H, s), 7.49 (2H, d, *J* = 8.2 Hz), 7.38-7.30 (3H, m), 7.27 (1H, s), 5.73 (1H, d, *J* = 16.5 Hz), 5.68 (1H, d, *J* = 16.1 Hz), 4.57 (1H, d, *J* = 14.8 Hz), 4.37 (1H, d, *J* = 14.8 Hz), 4.05-3.75 (8H, m), 3.45-3.15 (7H, m), 3.15-2.90 (2H, m), 2.18 (1H, m), 1.95 (1H, m); MS (FAB) *m/z* = 533 (M⁺ + H); HPLC purity = 98.7% (method B, 215 nm). Anal. (C₂₉H₃₃ClN₆O₂·3HCl·0.1CH₂Cl₂·0.3 EtOAc) C, H, N.

(S)-4-(5-[[1-(3-Chlorobenzyl)-2-oxopyrrolidin-3-yl]-(2-piperazin-1-ylethyl)amino)methyl]imidazol-1-ylmethyl)benzotrile Hydrochloride (54). A solution of aldehyde 51 (46 mg, 0.10 mmol), *N-tert*-butoxycarbonylpiperazine (22 mg, 0.12 mmol), and AcOH (17 μL, 0.30 mmol) in MeOH (2 mL) was stirred at ambient temperature for 30 min. NaCNBH₃ (13 mg, 0.20 mmol) was added and the reaction mixture was stirred for 48 h and then partitioned between saturated aqueous NaHCO₃ (10 mL) and CH₂Cl₂ (20 mL). The aqueous layer was extracted further with CH₂Cl₂ (2 × 20 mL), and the organic extracts were combined, dried with Na₂SO₄, filtered, and concentrated in vacuo. The crude product was purified via preparative HPLC (method A) and the product-containing fractions were lyophilized. The resulting trifluoroacetate salt was free-based and treated with HCl in EtOAc to afford the titled product (20 mg, 30%): ¹H NMR (CD₃OD) δ 9.15 (1H, s), 7.81 (2H, d, *J* = 8.4 Hz), 7.75 (1H, s), 7.51 (2H, d, *J* = 8.6 Hz), 7.37-7.30 (2H, m), 7.33 (1H, m), 7.17 (1H, m), 5.77 (1H, d, *J* = 16.1 Hz), 5.71 (1H, d, *J* = 15.9 Hz), 4.58 (1H, d, *J* = 15.0 Hz), 4.37 (1H, d, *J* = 14.7 Hz), 3.97 (1H, d, *J* = 15.6 Hz), 3.95 (1H, m), 3.86 (1H, d, *J* = 15.4 Hz), 3.65-3.45 (8H, m), 3.40-2.90 (6H, m), 2.15 (1H, m), 1.95 (1H, m); MS (FAB) *m/z* = 532 (M⁺ + H); HPLC purity = 95.0% (method B, 215 nm). Anal. (C₂₉H₃₄ClN₇O·4HCl·0.95H₂O) C, H, N.

Acknowledgment. The authors thank Walter F. Baginsky, Hema Bhimnathwala, Ian B. Greenberg, Kelly A. Hamilton, Hans E. Huber, Dongming Liu, Timothy J. O'Neill, and Ronald Robinson, for biological assaying of various compounds; Kenneth D. Anderson, Patrice A. Ciecko-Steck, Graham M. Smith, Bang-Lin Wan, and Matthew M. Zrada, for analytical chemistry support; Arthur B. Coddington, Harri G. Ramjit, and Charles W. Ross III, for mass spectral analyses; Michael J. Bogusky, Joan S. Murphy, Steven M. Pitzengerger, and Sandor L. Varga, for NMR spectroscopy expertise; Nigel J. Liverton, for helpful discussions; Neville Anthony, for critical reading of the manuscript; and Margaret Guttman, for manuscript preparation.

Supporting Information Available: Characterization data for all final compounds that are not described in the Experimental Section of this paper. This material is available free of charge via the Internet at <http://pubs.acs.org>.

References

- Bos, J. L. *Ras Oncogenes in Human Cancer: A Review. Cancer Res.* **1989**, *49*, 4682–4689.
- Gibbs, J. B. Ras C-Terminal Processing Enzymes—New Drug Targets. *Cell* **1991**, *65*, 1–4.
- Oliff, A. Farnesyltransferase Inhibitors: Targeting the Molecular Basis of Cancer. *Biochim. Biophys. Acta* **1999**, *1423*, C19–C30.
- Willumsen, B. M.; Norris, K.; Papageorge, A. G.; Hubbert, N. L.; Lowy, D. R. Harvey Murine Sarcoma Virus p21 Ras Protein: Biological and Biochemical Significance of the Cysteine Nearest the Carboxy Terminus. *EMBO J.* **1984**, *3*, 2581–2585.
- Casey, P. J.; Solski, P. A.; Der, C.; Buss, J. E. p21 Ras is Modified by a Farnesyl Isoprenoid. *Proc. Natl. Acad. Sci. U.S.A.* **1989**, *86*, 8323–8327.
- Bell, I. M. Inhibitors of Protein Prenylation 2000. *Exp. Opin. Ther. Patents* **2000**, *10*, 1813–1831.
- (a) Kohl, N. E.; Wilson, F. R.; Mosser, S. D.; Giuliani, E. A.; deSolms, S. J.; Conner, M. W.; Anthony, N. J.; Holtz, W. J.; Gomez, R. P.; Lee, T.-J.; Smith, R. L.; Graham, S. L.; Hartman, G. D.; Gibbs, J. B.; Oliff, A. Protein Farnesyltransferase Inhibitors Block the Growth of *ras*-Dependent Tumors in Nude Mice. *Proc. Natl. Acad. Sci. U.S.A.* **1994**, *91*, 9141–9145. (b) Qian, Y.; Blaskovich, M. A.; Seong, C.-M.; Vogt, A.; Hamilton, A. D.; Sebti, S. M. Peptidomimetic Inhibitors of p21Ras Farnesyltransferase: Hydrophobic Functionalization Leads to Disruption of p21Ras Membrane Association in Whole Cells. *Bioorg. Med. Chem. Lett.* **1994**, *4*, 2579–2584.
- (a) Singh, S. B.; Zink, D. L.; Liesch, J. M.; Goetz, M. A.; Jenkins, R. G.; Nallin-Omstead, M.; Silverman, K. C.; Bills, G. F.; Mosley, R. T.; Gibbs, J. B.; Albers-Schonberg, G.; Lingham, R. B. Isolation and Structure of Chaetomelic Acids A and B from *Chaetomella acutisetata*—Farnesyl Pyrophosphate Mimic Inhibitors of Ras Farnesylprotein Transferase. *Tetrahedron* **1993**, *49*, 5917–5926. (b) Dabrah, T. T.; Harwood, H. J.; Huang, L. H.; Jankovich, N. D.; Kaneko, T.; Li, J.-C.; Lindsey, S.; Moshier, P. M.; Subashi, T. A.; Therrien, M.; Watts, P. C. CP-225,917 and CP-263, 114, Novel Ras Farnesylation Inhibitors from an Unidentified Fungus. I. Taxonomy, Fermentation, Isolation, and Biochemical Properties. *J. Antibiot.* **1997**, *50*, 1–7.
- (a) Pompliano, D. L.; Rands, E.; Schaber, M. D.; Mosser, S. D.; Anthony, N. J.; Gibbs, J. B. Steady-state Kinetic Mechanism of Ras Farnesylprotein Transferase. *Biochemistry* **1992**, *31*, 3800–3807. (b) Patel, D. V.; Schmidt, R. J.; Biller, S. A.; Gordon, E. M.; Robinson, S. S.; Manne, V. Farnesyl Diphosphate-Based Inhibitors of Ras Farnesyl-Protein Transferase. *J. Med. Chem.* **1995**, *38*, 2906–2921.
- (a) End, D.; Skrzat, S.; Devine, A.; et al. R115777, a Novel Farnesyl Protein Transferase Inhibitor (FTI): Biochemical and Cellular Effects in H-Ras and K-Ras Dominant Systems. *Proc. Am. Assoc. Cancer Res.* **1998**, *39*, 270. Abstract 1847. (b) Njoroge, F. G.; Taveras, A. G.; Kelly, J.; Temiszewski, S.; Mallams, A. K.; Wolin, R.; Afonso, A.; Cooper, A. B.; Rane, D. F.; Liu, Y. T.; Wong, J.; Vibulhan, B.; Pinto, P.; Desku, J.; Alvarez, C. S.; del Rosario, J.; Connolly, M.; Wang, J.; Desai, J.; Rossman, R. R.; Bishop, W. R.; Patton, R.; Wang, L.; Kirschmeier, P.; Ganguy, A. K. (+)-4-[2-[4-(8-Chloro-3,10-dibromo-6,11-dihydro-5H-benzo[5,6]cyclohepta[1,2-b]pyridin-11(R)-yl]-1-piperidinyl]-2-oxoethyl]-1-piperidinecarboxamide (SCH-66336). A Very Potent Farnesyl Protein Transferase Inhibitor as a Novel Antitumor Agent. *J. Med. Chem.* **1998**, *41*, 4890–4902.
- Williams, T. M.; Bergman, J. M.; Brashear, K.; Breslin, M. J.; Dinsmore, C. J.; Hutchinson, J. H.; MacTough, S. C.; Stump, C. A.; Wei, D. D.; Zartman, C. B.; Bogusky, M. J.; Culbertson, J. C.; Buser-Doepner, C.; Davide, J.; Greenberg, I. B.; Hamilton, K. A.; Koblan, K. S.; Kohl, N. E.; Liu, D.; Lobell, R. B.; Mosser, S. D.; O'Neill, T. J.; Rands, E.; Schaber, M. D.; Wilson, F.; Senderak, E.; Motzel, S. L.; Gibbs, J. B.; Graham, S. L.; Heimbrook, D. C.; Hartman, G. D.; Oliff, A. I.; Huff, J. R. *N*-Arylpiperazinone Inhibitors of Farnesyltransferase: Discovery and Biological Activity. *J. Med. Chem.* **1999**, *42*, 3779–3784.
- Freidinger, R. M.; Veber, D. F.; Perlow, D. S.; Brooks, J. R.; Saperstein, R. Bioactive Conformation of Luteinizing Hormone-Releasing Hormone: Evidence from a Conformationally Constrained Analogue. *Science* **1980**, *210*, 656–658.
- Aube, J. Synthetic Routes to Lactam Peptidomimetics. *Adv. Amino Acid Mimetics Peptidomimetics* **1997**, *1*, 193–232.
- Koblan, K. S.; Culbertson, J. C.; deSolms, S. J.; Giuliani, E. A.; Mosser, S. D.; Omer, C. A.; Pitzengerger, S. M.; Bogusky, M. J. NMR Studies of Novel Inhibitors Bound to Farnesyl-Protein Transferase. *Protein Sci.* **1995**, *4*, 681–688.
- Freidinger, R. M.; Perlow, D. S.; Veber, D. F. Protected Lactam-Bridged Dipeptides for Use as Conformational Constraints in Peptides. *J. Org. Chem.* **1982**, *47*, 104–109.
- Anthony, N. J.; Gomez, R. P.; Schaber, M. D.; Mosser, S. D.; Hamilton, K. A.; O'Neill, T. J.; Koblan, K. S.; Graham, S. L.; Hartman, G. D.; Shah, D.; Rands, E.; Kohl, N. E.; Gibbs, J. B.; Oliff, A. I. Design and In Vivo Analysis of Potent Non-Thiol Inhibitors of Farnesyl Protein Transferase. *J. Med. Chem.* **1999**, *42*, 3356–3368.
- Bell, I. M.; Beshore, D. C.; Gallicchio, S. N.; Williams, T. M. Efficient Synthesis of 1-Heterocyclic-3-aminopyrrolidinones. *Tetrahedron Lett.* **2000**, *41*, 1141–1145.
- Weissman, S. A.; Lewis, S.; Askin, D.; Volante, R. P.; Reider, P. J. Efficient Synthesis of *N*-Arylpiperazinones via a Selective Intramolecular Mitsunobu Cyclodehydration. *Tetrahedron Lett.* **1998**, *39*, 7459–7462.
- Aszodi, J.; Bonnet, A.; Teutsch, G. Enantioselective Synthesis of a Versatile 2-Isocephem Synthone. *Tetrahedron* **1990**, *46*, 1579–1586.
- Omura, K.; Swern, D. Oxidation of Alcohols by “Activated” Dimethyl Sulfoxide. A Preparative, Steric and Mechanistic Study. *Tetrahedron* **1978**, *34*, 1651–1660.
- Omer, C. A.; Kral, A. M.; Diehl, R. E.; Prendegast, G. C.; Powers, S.; Allen, C. M.; Gibbs, J. B.; Kohl, N. E. Characterization of Recombinant Human Farnesyl-Protein Transferase: Cloning, Expression, Farnesyl Diphosphate Binding, and Functional Homology with Yeast Prenyl-Protein Transferases. *Biochemistry* **1993**, *32*, 5167–5176.
- Temeles, G. L.; Gibbs, J. B.; D'Alonzo, J. S.; Sigal, I. S.; Scolnick, E. M. Yeast and Mammalian Ras Proteins Have Conserved Biochemical Properties. *Nature (London)* **1985**, *313*, 700–703.
- U. S. Patent No. 5,470,832.
- Huber, H. E.; Robinson, R.; Watkins, A.; Nahas, D.; Abrams, M.; Buser, C.; Lobell, R.; Patrick, D.; Anthony, N.; Dinsmore, C.; Graham, S.; Hartman, G.; Lumma, W.; Williams, T.; Heimbrook, D. C. Anions Modulate the Potency of Geranylgeranyl-Protein Transferase-I Inhibitors. *J. Biol. Chem.* In press.
- Fiset, C.; Feng, Z.-P.; Wang, L.; Sheldon, R. S.; Duff, H. J. [³H]-Dofetilide Binding: Biological Models that Manifest Solely the High or the Low Affinity Binding Site. *J. Mol. Cell. Cardiol.* **1996**, *28*, 1085–1096.
- Zhou, Z.; Gong, Q.; Ye, B.; Fan, Z.; Makielski, J. C.; Robertson, G. A.; January, C. T. Properties of HERG Channels Stably Expressed in HEK 293 Cells Studied at Physiological Temperature. *Biophys. J.* **1998**, *74*, 230–241.
- Claremont, D. A.; Baldwin, J. J.; Elliott, J. M.; Remy, D. C.; Ponticello, G. S.; Selnick, H. G.; Lynch, J. J., Jr.; Sanguinetti, M. C.; Selective I_{Kr} Potassium Channel Blockers as Class III Antiarrhythmic Agents. In *Perspectives in Medicinal Chemistry*; Testa, B., Kyburz, E., Fuhrer, W., Giger, R., Eds.; Verlag Helvetica Chimica Acta: Basel, 1993; pp 389–404.
- Fukazawa, H.; Nakano, S.; Mizuno, S.; Uehara, Y. Inhibitors of Anchorage-Independent Growth Affect the Growth of Transformed Cells on Poly(2-hydroxyethyl methacrylate)-Coated Surfaces. *Int. J. Cancer* **1996**, *67*, 876–882.
- Kohl, N. E.; Mosser, S. D.; deSolms, S. J.; Giuliani, E. A.; Pompliano, D. L.; Graham, S. L.; Smith, R. L.; Scolnick, E. M.; Oliff, A. I.; Gibbs, J. B. Selective Inhibition of Ras-Dependent Transformation by a Farnesyltransferase Inhibitor. *Science* **1993**, *260*, 1934–1937.
- Mossman, T. Rapid Colorimetric Assay for Cellular Growth and Survival: Application to Proliferation and Cytotoxicity Assays. *J. Immunol. Methods* **1983**, *65*, 55–63.
- Omer, C. A.; Chen, Z.; Diehl, R. E.; Connor, M. W.; Chen, H. Y.; Trumbauer, M. E.; Gopal-Truter, S.; Seeburger, G.; Bhimnathwala, H.; Abrams, M. T.; Davide, J. P.; Ellis, M. S.; Gibbs, J. B.; Greenberg, I.; Hamilton, K.; Koblan, K. S.; Kral, A. M.; Liu, D.; Lobell, R. B.; Miller, P. J.; Mosser, S. D.; O'Neill, T. J.; Rands,

- E.; Schaber, M. D.; Senderak, E. T.; Oliff, A.; Kohl, N. E. Mouse Mammary Tumor Virus-Ki-rasB Transgenic Mice Develop Mammary Carcinomas That Can Be Growth-Inhibited by a Farnesyl: Protein Transferase Inhibitor. *Cancer Res.* **2000**, *60*, 2680–2688.
- (32) Williams, T. M. et al. Manuscript in preparation.
- (33) Bellamy, W. T. P-Glycoproteins and Multidrug Resistance. *Annu. Rev. Pharmacol. Toxicol.* **1996**, *36*, 161–183.
- (34) Lobell, R. B.; Kohl, N. E. Unpublished results.
- (35) Netzer, R.; Ebnet, A.; Bischoff, U.; Pongs, O. Screening Lead Compounds for QT Interval Prolongation. *Drug Discov. Today* **2001**, *6*, 78–84.
- (36) Sanguinetti, M. C.; Keating, M. T. Role of Delayed Rectifier Potassium Channels in Cardiac Repolarization and Arrhythmias. *News Physiol. Sci.* **1997**, *12*, 152–157.
- (37) Williams, T. M.; Ciccarone, T. M.; MacTough, S. C.; Bock, R. L.; Conner, M. W.; Davide, J. P.; Hamilton, K.; Koblan, K. S.; Kohl, N. E.; Kral, A. M.; Mosser, S. D.; Omer, C. A.; Pompliano, D. L.; Rands, E.; Schaber, M. D.; Shah, D.; Wilson, F. R.; Gibbs, J. B.; Graham, S. L.; Hartman, G. D.; Oliff, A. I.; Smith, R. L. 2-Substituted Piperazines as Constrained Amino Acids. Application to the Synthesis of Potent, Non Carboxylic Acid Inhibitors of Farnesyltransferase. *J. Med. Chem.* **1996**, *39*, 1345–1348.
- (38) Sepp-Lorenzino, L.; Ma, Z.; Rands, E.; Kohl, N.; Gibbs, J. B.; Oliff, A.; Rosen, N. A Peptidomimetic Inhibitor of Farnesyl: Protein Transferase Blocks the Anchorage-dependent and Independent Growth of Human Tumor Cell Lines. *Cancer Res.* **1995**, *55*, 5302–5309.
- (39) Sun, J.; Quian, Y.; Hamilton, A. D.; Sebti, S. M. Both Farnesyltransferase and Geranylgeranyltransferase I Inhibitors Are Required for Inhibition of Oncogenic K-ras Prenylation But Each Alone is Sufficient to Suppress Human Tumor Growth in Nude Mouse Xenografts. *Oncogene* **1998**, *16*, 1467–1473.
- (40) Prendergast, G. C. Farnesyltransferase Inhibitors: Antineoplastic Mechanism and Clinical Prospects. *Curr. Opin. Cell Biol.* **2000**, *12*, 166–173.
- (41) Ashar, H. R.; James, L.; Gray, K.; Carr, D.; Black, S.; Armstrong, L.; Bishop, W. R.; Kirschmeier, P. Farnesyl Transferase Inhibitors Block the Farnesylation of CENP-E and CENP-F and Alter the Association of CENP-E with the Microtubules. *J. Biol. Chem.* **2000**, *275*, 30451–30457.
- (42) Ferraccioli, R.; Croce, P. D.; Gallina, C.; Consalvi, V.; Scandurra, R. Synthesis and Inhibiting Properties Toward Trypsin Like Proteases of *N* α -(*N,N*-Dimethylcarbamoyl)- α -azalysine and α -Azalysine Esters. *Farmaco* **1991**, *46*, 1517–1531.
- (43) Kearsley, S., Merck & Co., Inc., unpublished results.
- (44) Beese, L. S.; Taylor, J. S., unpublished results.
- (45) Mohamadi, F.; Richards, N. G. J.; Guida, W. C.; Liskamp, R.; Lipton, M.; Cauffield, C.; Chang, G.; Hendrickson, T.; Still, W. C. Macromodel—An Integrated Software System for Modeling Organic and Bioorganic Molecules Using Molecular Mechanics. *J. Comput. Chem.* **1990**, *11*, 440–467.

JM010156P